

Air Force Institute of Technology

AFIT Scholar

Theses and Dissertations

Student Graduate Works

12-1996

Investigation of Sorption Mass Transfer Models Using Synthetic Soils

Karla K. Mika

Follow this and additional works at: <https://scholar.afit.edu/etd>



Part of the [Environmental Engineering Commons](#)

Recommended Citation

Mika, Karla K., "Investigation of Sorption Mass Transfer Models Using Synthetic Soils" (1996). *Theses and Dissertations*. 5908.

<https://scholar.afit.edu/etd/5908>

This Thesis is brought to you for free and open access by the Student Graduate Works at AFIT Scholar. It has been accepted for inclusion in Theses and Dissertations by an authorized administrator of AFIT Scholar. For more information, please contact AFIT.ENWL.Repository@us.af.mil.



**INVESTIGATION OF
SORPTION MASS TRANSFER MODELS
USING SYNTHETIC SOILS**

THESIS

Karla K. Mika, Captain, USAF

AFIT/GEE/ENV/96D-13

19970205 024

DEPARTMENT OF THE AIR FORCE

DTIC QUALITY INSPECTED 3

AIR UNIVERSITY

AIR FORCE INSTITUTE OF TECHNOLOGY

Wright-Patterson Air Force Base, Ohio

DISTRIBUTION STATEMENT A

**Approved for public release;
Distribution Unlimited**

E

AFIT/GEE/ENV/96D-13

**INVESTIGATION OF
SORPTION MASS TRANSFER MODELS
USING SYNTHETIC SOILS**

THESIS

Karla K. Mika, Captain, USAF

AFIT/GEE/ENV/96D-13

DTIC QUALITY INSPECTED 3

Approved for public release; distribution unlimited

The views expressed in this thesis are those of the author and do not reflect the official policy or position of the Department of Defense or the U.S. Government.

AFIT/GEE/ENV/96D-13

**INVESTIGATION OF
SORPTION MASS TRANSFER MODELS
USING SYNTHETIC SOILS**

THESIS

**Presented to the Faculty of the School of Engineering
of the Air Force Institute of Technology
in Partial Fulfillment of the
Requirements for the Degree of
Master of Science in Engineering and Environmental Management**

Karla K. Mika, BS

Captain, USAF

December 1996

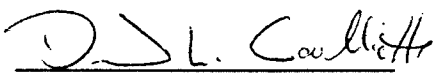
Approved for public release; distribution unlimited


**INVESTIGATION OF
SORPTION MASS TRANSFER MODELS
USING SYNTHETIC SOILS**

THESIS

**Presented to the Faculty of the School of Engineering
of the Air Force Institute of Technology
in Partial Fulfillment of the
Requirements for the Degree of
Master of Science in Engineering and Environmental Management**


Co-Chairman


Co-Chairman


Member

Acknowledgments

I am appreciative of my advisors, Lieutenant Colonel Dave Coulliette and Major Ed Heyse, who were generous with their help in my research effort.

My thanks to Major Heyse for the conceptual basis of my research. Without his ingenuity and foresight, my research would have lacked direction and effect. His intuitive approach to advising allowed me the freedom to learn the concepts at my own pace and the creativity to assimilate the knowledge in my own way. Still, his ability to assess experimental design and model analysis kept me on task.

Thanks also to Lieutenant Colonel Coulliette whose work with Major Heyse on the model code kept me from overstepping the limits of my mathematical and programming abilities.

In addition, I would like to thank the third member of my thesis committee, Major Jeff Martin, whose stable guidance helped to calm my intermittent anxieties due to instrument difficulties.

I truly appreciate the work by fellow master's degree candidate, Captain Tom deVenoge; he was always one experiment, analysis, or model run ahead of me. I thank him for the opportunity to observe. I also thank him for always accompanying me during the grueling discussions regarding the model with Major Heyse.

I am grateful to Dr. Mark Goltz for his useful comments regarding my review of the literature. His comments served to enhance the readability of my review as well as the accuracy.

I would like to express my appreciation to P. S. C. Rao and Dongping Dai, University of Florida, Gainesville, for providing the porous ceramic spheres used in this study.

Certainly, I wish to thank the Air Force Institute of Technology for the opportunity to obtain yet another degree at their expense. Research funding for this work was provided by the Air Force Office of Scientific Research.

Finally, I could not have done this work without the constant support of my family: my husband, Dan, and my children, Jase and Kate. I am constantly reminded of how blessed I am to have a husband who shares my interests and aspirations. Without Dan's knowledge of analytical chemistry, my laboratory experiments and subsequent analysis would have suffered greatly. It is with extreme gratitude that I acknowledge how important he is in my life. Also, a special thanks to my children, for the sacrifices they have made and for the unconditional love and trust they place in me. The responsibility that comes with parenting is immense; my hope is that my efforts here help to exemplify for them the virtues of education, hard-work and perseverance.

Karla K. Mika

Table of Contents

	Page
ACKNOWLEDGMENTS	ii
LIST OF FIGURES	v
LIST OF TABLES	vi
ABSTRACT.....	vii
I. INTRODUCTION	1
OVERVIEW OF RESEARCH INTEREST	1
RESEARCH OBJECTIVES	2
II. REVIEW OF THE LITERATURE.....	3
SORPTION FUNDAMENTALS	3
SORBENT DISTRIBUTION	6
SORPTION MODELS	10
SORPTION STUDIES INVOLVING SYNTHETIC MEDIA	21
III. METHODOLOGY	24
MATERIALS.....	24
EXPERIEMENTS	26
IV. DATA ANALYSIS AND MODEL SIMULATION.....	30
EXPERIMENTAL DATA ANALYSIS.....	30
MODEL SIMULATION AND ANALYSIS	41
V. SUMMARY AND CONCLUSION.....	49
VI. REFERENCES.....	50
APPENDIX A: GLOSSARY	56
APPENDIX B: EXPERIMENT DATA.....	58
APPENDIX C: MSS MODEL CODE	60
APPENDIX D: MSS MODEL INPUT DATA	86
VITA.....	110

List of Figures

	Page
FIGURE	
1. TWO-SITE AND MSS MASS TRANSFER MODELS.....	18
2. UPTAKE OF ANTHRACENE BY NYLON 66 (PARTITIONING BASIS).....	31
3. UPTAKE OF ANTHRACENE BY NYLON 66 (ADSORPTION BASIS).....	32
4. UPTAKE OF ANTHRACENE BY PARAFFIN (PARTITIONING BASIS).....	34
5. UPTAKE OF ANTHRACENE BY PARAFFIN (ADSORPTION BASIS).....	35
6. UPTAKE OF ANTHRACENE BY POROUS CERAMIC SPHERES	37
7. UPTAKE OF ANTHRACENE BY CERAMIC AND PARAFFIN SPHERES.....	38
8. TRUE "VIRTUAL" GEOMETRY CREATED FROM COMPOSITE OF PARAFFIN AND POROUS CERAMIC SPHERES	47
9. TRUE AND FITTED DISTRIBUTIONS OF SORPTION CAPACITY FOR MIXED MEDIA EXPERIMENTS.....	48

List of Tables

	Page
TABLE	
1. NYLON-66 ISOTHERM EXPERIMENT	60
2. NYLON-66 RATE EXPERIMENT	60
3. POROUS CERAMIC SPHERE RATE EXPERIMENT	60
4. MIXED POROUS CERAMIC AND PARAFFIN SPHERE RATE EXPERIMENT	61
5. FIT DEFF USING KNOWN δ_{MAX} AND λ	42
6. EFFECTIVE DIFFUSION COEFFICIENTS FOR NONSORBING SOLUTES INTO 0.75 CM DIA. POROUS CERAMIC SPHERES	43
7. TWO-PARAMETER FIT, δ AND λ , USING FREE-LIQUID DIFFUSION COEFFICIENT, D_o	45

Abstract

Grain-scale sorption mass transfer is an important process that must be considered when predicting clean-up time and choosing remediation techniques for subsurface hazardous waste contamination. Rate-limited sorption is responsible for the rebound effect, where remediated groundwater is recontaminated by desorption. Sorbed contaminants are not available for microbial degradation, and the desorption rate may govern the effectiveness of natural attenuation by biodegradation. Grain-scale sorption nonequilibrium is generally attributed to diffusive transport, either in soil organic matter or in mineral micropores. Typically used sorption mass transfer models either fail to reproduce long-term slow desorption (first-order models), or are based on diffusion in assumed (often spherical) grain geometries. New multisite models have been proposed that incorporate more realistic grain geometries. To validate these models, we have conducted sorption rate experiments with paraffin, nylon, and porous ceramic spheres. These synthetic surrogate soils were chosen for their differing, but known, sorption coefficients, diffusion coefficients, and geometries. Experiments were conducted in batch systems containing only a single material and size, as well as distributions of two or more materials and sizes. We tested the ability of the model to simulate the behavior of these systems and to fit system parameters from rate data.

INVESTIGATION OF SORPTION MASS TRANSFER MODELS USING SYNTHETIC SOILS

I. Introduction

Overview of Research Interest:

Chemicals released into the subsurface move through the soil and often contaminate the groundwater. Hydrophobic organic chemicals (HOCs) such as chlorinated solvents and fuel components released at many Air Force installations are of concern because these chemicals may possess mutagenic, teratogenic, and/or carcinogenic properties. The processes that affect the transport and fate of these contaminants must be understood in order to assess exposure risks to humans and the environment and to develop efficient and cost-effective remediation strategies.

The transport, distribution, fate and biological availability of many HOCs in the groundwater are highly dependent on sorption by aquifer solids; therefore, understanding sorption phenomena between solute and sorbent is critical. Although sorption is often considered to be an instantaneous process for modeling purposes, sorption and desorption may not always be fast compared to other fate or transport processes such as advection and dispersion. Studies indicate the time the aquifer solids are exposed to the solute even at low flow rates may not be long enough to permit complete sorption equilibrium (Roberts et al., 1986; Ball and Roberts, 1991a, Brusseau and Rao, 1991a). Equilibrium sorption expressions are not always able to predict the results observed in experimental studies (van Genuchten et al., 1974). Sorption nonequilibrium exists in part because mass transfer between moving groundwater and soil organic matter (SOM) is governed by

diffusion. This physical nonequilibrium can have marked effects on chemical transport resulting in breakthrough curves (concentration versus time profiles at a point in space) that have earlier arrivals and longer "tails" than would be predicted assuming equilibrium sorption (Weber et al., 1991). Nonequilibrium sorption within individual soil grains has been found to greatly affect the rate of biotransformation (Ramaswami et al., 1994) by limiting the degree to which the contaminant is bioavailable (Scow and Alexander, 1992). Bioavailability is important because it often accounts for the persistence of compounds that are biodegradable and might otherwise readily decompose (Alexander, 1994). Knowledge of sorption phenomena will improve the ability to predict contaminant mobility and bioavailability. By improving sorption mass transfer models, more accurate exposure and risk estimates for groundwater pollutants and improved clean-up operations are possible. New models developed for this purpose require rigorous testing using media of known properties that affect sorption sites (Heyse, 1994). Experiments using synthetic media with known geometries and sorption characteristics must be made to test model validity.

Research Objectives:

The purpose of this experimental study is to test a theory that relates sorption rate to geometry of sorbent particles. Specifically, this research seeks to determine if a heterogeneous distribution of diffusion domains can be described by one average geometry, and to determine if that average geometry can be predicted from experimental sorption rate data.

II. Review of the Literature

Sorption Fundamentals:

Sorption is the process by which the solutes in the liquid phase associate with the sorbent or solid phase. The chemical structure of a molecule and the nature of the solid phase play large roles in determining the extent of sorption. Sorption is used to indicate both adsorption onto a two-dimensional surface, and absorption into a three-dimensional matrix (Schwarzenbach et al., 1993). Adsorption is the accumulation occurring at an interface while absorption is the partitioning between two phases, and sorption includes both adsorption and absorption. With absorption the equilibrium partition coefficient (K_p) quantifies the solute distribution in the aqueous and solid phases.

For nonpolar organic contaminants, sorption is dependent on the hydrophobicity of the compound. The HOC in this study is a neutral nonpolar organic compound where the partition coefficient is represented by Equation (1) (Karickhoff, et al., 1979):

$$K_p = \frac{X}{C_l} \quad (1)$$

with

$$X = C_{om}f_{om} + \frac{C_{im}\theta_{im}}{\rho_B} \quad (2)$$

where:

X = sorbed phase concentration in the organic matter and the micropores,

C_{om} = concentration of sorbate associated with the SOM,

f_{om} = weight fraction of solid which is SOM,

C_{im} = average aqueous immobile phase concentration,

θ_{im} = immobile phase porosity, and

C_i = concentration of solute in solution.

For hydrophobic compounds, the fraction of organic matter of the subsurface solid phase is the dominant soil characteristic affecting sorption. Studies indicate that many HOCs are sorbed primarily by organic matter (Karickhoff et al., 1979; Chiou et al., 1983; Gschwend and Wu, 1985; Rutherford et al., 1992). Sorption can be viewed as partitioning into the organic matter rather than as sorption onto the sorbent surface (Karickhoff, 1981; Chiou et al., 1979). Chiou et al. (1979, 1983) have described SOM sorption as a partitioning process due to the polymer-like structure of soil organic matter. Normalization of the K_p values by f_{oc} results in a parameter, organic carbon distribution coefficient (K_{oc}) (Karickhoff, 1981). The K_{oc} is independent of the soil and a function only of the chemical. K_p is proportional to the f_{oc} with K_{oc} being the proportionality constant as shown in Equation (3):

$$K_p = \frac{K_{oc}}{f_{oc}} \quad (3)$$

Studies to support the relationship shown include Miller and Weber (1986) who noted significant decreases in sorption when the organic content of the soil was removed. Typical values for f_{oc} for surface soils range from 0.01 to 0.08 (Hamaker and Thompson, 1972) and 0.0002 to 0.01 for alluvial sand aquifer materials (Schwarzenbach and Westall, 1981).

Equation (3) demonstrates that K_p can be computed by measuring the f_{oc} of the subsurface material and selecting a value of K_{oc} . The value of K_{oc} can be estimated from the octanol-water partition coefficient (K_{ow}). K_{ow} describes the partitioning of an organic chemical between a polar phase (water) and a relatively nonpolar phase (1-octanol). Karickhoff et al. (1979) proposed that the octanol-water partitioning closely parallels the sorption in the soil system. Since, several researchers have proposed empirical expressions to relate K_{oc} to either the water solubility or K_{ow} of a chemical (Karickhoff et al., 1979; Chiou et al., 1983; Schwarzenbach and Westall, 1981). These empirical relationships assumed the porous medium to be saturated with water. Deviations in sorption have been observed when the soil is dehydrated and when an organic solvent is present in place of the water. Chiou et al. (1985) demonstrated in aqueous systems that the water molecules compete with the solute for sorption sites on mineral surfaces. They found that as the medium is dehydrated, more of the organics are able to sorb onto the mineral surfaces. Also, in the presence of organic solvents, the solute is highly soluble; thus, the sorption of the solute significantly decreases.

Sorbent Distribution:

Sorption of solute into the sorbent matrix is not fully understood. In order to predict sorption behavior, it is important to conceptualize the mechanism by which the sorbent, the soil organic matter, retains the HOC molecules. SOM has been described to exist in three geometries; as discrete particles, as surface coatings, or within micropores of mineral grains (Augustijn, 1993). Each of the three organic matter geometries is likely to exist in soils with the most abundant controlling the sorptive process. Hydrophobic molecule diffusion into SOM has been used to explain rate limited sorption. Diffusive transport is caused by random molecular movement of solute from areas of high concentration to areas of low concentration (Crank, 1975). Fick's first law quantifies diffusion by the mathematical equation (Equation (4)):

$$J = -D \frac{\partial C}{\partial x} \quad (4)$$

where:

J = mass flux of individual components,

D = diffusion coefficient,

C = concentration of individual components, and

x = distance.

The magnitude of the molecular motion is determined by the internal energy of the solute molecule, dependent on temperature, and represented by the diffusion coefficient (Szecsody, 1988). The diffusion of an aqueous solute in the subsurface is a very slow

process with diffusion coefficients on the order of 10^{-5} or 10^{-6} cm^2/s for most fuel constituents (Schwarzenbach et al., 1993).

Rate limited sorption may be explained using either the intraorganic matter diffusion, IOMD, theory (Karickhoff and Morris, 1985) or by the retarded intraparticle diffusion (RIPD) theory (Miller and Weber, 1984, 1986; Ball and Roberts, 1991b). Each theory was developed through experimental observations under differing conditions that might serve to explain the differing theoretical conclusions.

The IOMD theory of sorption mass transfer likens SOM to a polymer matrix. In IOMD nonequilibrium is caused by diffusion limitations into the polymer-like matrix of SOM. Diffusion path lengths in the SOM matrix can be high enough to cause significant mass transfer limitations. Lee et al. (1988) investigated the movement of TCE and p-xylene in two sand aquifer materials and concluded that the nonequilibrium was indeed caused by diffusion imitations into the organic matter matrix of the soils. The diffusion path is not a simple straight line but a tortuous path between the polymer-like humic molecules. The longer, tortuous path results in longer times for a molecule to diffuse into or out of SOM. Longer path lengths would indicate increased diffusion limitations and decreased sorption rates. Brusseau et al. (1991b) and Woodburn et al. (1989) proposed that organic cosolvents increase the rate of sorption due to their ability to swell SOM, thus increasing path length. The researchers conducted batch and transport experiments to measure sorption of polyaromatic hydrocarbons (PAHs) on Webster soil from 30/70 (v/v) and 50/50 (v/v) methanol/water mixtures. The studies indicate that the dominant mechanism for sorption was similar to the mechanism for retention of PAHs by reverse

phase liquid chromatography (RPLC). RPLC packing material is known to swell when used as a sorbent material, and when used with a cosolvent mixture the rate of sorption is increased. Carroll et al., (1994) investigated diffusion of PCBs from the swollen and condensed phases of the Hudson River sediment organic matter using a permeant/polymer diffusion model. Data from long-term PCB desorption were fit and equivalent diameters for swollen and condensed humic polymer were estimated. A 3-fold difference in diameter is obtained for the swollen humic polymer, while values for the condensed polymer are virtually identical. The larger diameter of the swollen humic polymer results in longer path lengths which would indicate increased diffusion limitations and decreased sorption rates.

Gauthier et al. (1987) purport the major cause of variations in the observed coefficients to be related to the structural characteristics of the SOM. They found the magnitude of the K_{oc} values correlated strongly with the degree of aromaticity in the humic material. Their analysis indicates a decrease in rate for polar molecules capable of hydrogen bonding within SOM supports IOMD.

Retarded intraparticle diffusion is conceptually described as sorption in micropores. Like IOMD, RIPD has also been postulated as a possible mechanism for rate-limited sorption (Miller and Weber, 1984, 1986; Wu and Gschwend, 1986; Ball and Roberts, 1991b). In contrast to the flexible pore network in SOM visualized by IOMD, the micropores of RIPD are thought to be rigid and permanent. The RIPD geometry is characterized by long, tortuous diffusion path lengths. Slow mass transfer is the result of retardation by sorption to SOM in the micropores and steric hindrance and constrictivity between the advective and diffusive domains of the micropores. Wu and Gschwend

(1986) found that large particles showed a slower approach to equilibrium than smaller but otherwise similar particles using the same sorbate. By reducing the diffusive path length into the interior of the particles and by increasing exposed sorbent surface area, they were able to increase sorption rate. Steinberg et al. (1987) mechanically broke soil particles in a ball mill and observed an increase in the rate of desorption. Apparently, the reduction in pore path length by pulverization induced faster rates. Similarly, Ball and Roberts (1991a) analyzed the long-term sorption of tetrachloroethene (PCE) and 1,2,4,5-tetrachlorobenzene (TeCB) by aquifer solids and found increases in rate with particle pulverization giving evidence of RIPD.

Both the RIPD and IOMD theories maintain that diffusion can be used to explain rate limited sorption, and it may be that both IOMD and RIPD mechanisms exist in the environment, possibly in the same particle. The predominate mechanism in soils that are high in SOM appears to be IOMD, while RIPD may predominate in soils of low SOM content or soils which have grain-scale mineral microporosity.

Sorption Models:

Mass transfer rate limitations are often modeled using either diffusion (second-order) models or first-order approximations of diffusion.

First-Order Models

Early physical nonequilibrium modeling used a comparatively simple first-order rate expression to describe transfer of contaminant between regions of mobile and immobile water. van Genuchten and Wierenga (1976) described the mass transfer of solute in sorbing porous media by dividing the porous media into four domains: (1) mobile (turbulent) water located in the larger (inter-aggregate) pores, (2) immobile (stagnant) water located inside aggregates and at the contact points of aggregates and/or particles, (3) dynamic soil, located sufficiently close to the mobile water phase so that equilibrium could be assumed to exist between solute in the mobile water phase and the soil phase, and (4) stagnant soil where equilibrium could be assumed to exist between solute in the immobile water phase and the soil phase. The diffusive rate-limitations in this model comes from the first-order rate expression that describes transfer of contaminant between mobile and immobile water regions.

Based on these assumptions, Equation (5) was developed to represent transport between the domains (van Genuchten and Wierenga, 1976)

$$(\theta_m + f\rho_b K_d) \frac{\partial C_m}{\partial t} + [\theta_{im} + (1-f)\rho_b K_d] \frac{\partial \bar{C}_{im}}{\partial t} = \theta_m D_m \frac{\partial^2 C_m}{\partial x^2} - \theta_m v \frac{\partial C_m}{\partial x} \quad (5)$$

where:

C_m = concentration in the mobile liquid phase,

\overline{C}_{im} = average concentration in the immobile liquid phase,

θ_m = mobile phase porosity,

θ_{im} = immobile phase porosity,

f = fraction of sorption sites that are in contact with the mobile liquid phase,

ρ_b = bulk soil density,

K_d = linear sorption distribution coefficient,

D_m = mobile region dispersion coefficient,

v = average pore water velocity, and

t = time.

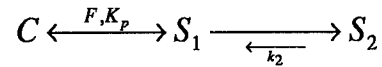
The mass transfer between the mobile and immobile phases was considered to be first-order modeled as Equation (6):

$$[\theta_{im} + (1-f)\rho_b K_d] \frac{\partial \overline{C}_{im}}{\partial t} = \alpha' (C_m - \overline{C}_{im}) \quad (6)$$

where:

α' = first-order mass transfer coefficient.

A modification of the approach described above is the two-site sorption kinetic model that is characterized by two sorptive sites, S_1 and S_2 (Brusseau and Rao, 1989). The S_1 sites are equilibrium sites where the solid phase rapidly equilibrates with the solution phase. The S_2 sites are rate-limited sites where sorption between the aqueous and solid phase is described by a first-order rate equation (van Genuchten and Wagenet, 1989). This model can be visualized as



where:

C = mass of solute dissolved in the liquid phase

S = mass of solute sorbed per mass of sorbent

F = fraction of sorbent for which sorption is instantaneous

k_2 = first-order mass transfer rate coefficient

This model is described mathematically by Equations (7) - (9):

$$S = S_1 + S_2 \quad (7)$$

$$S_1 = FK_p C \quad (8)$$

$$\frac{dS_2}{dt} = k_2 (K_p C (1 - F) - S_2). \quad (9)$$

Nkedi-Kizza et al. (1989) show the two-site model is mathematically equivalent to the van Genuchten and Wierenga (1976) model. The three parameters needed to model two-site mass transfer are the equilibrium partition coefficient, K_p , the fraction of equilibrium sites, F , and the desorption rate coefficient for the slow sites, k_2 . The partition coefficient can be obtained independently through batch isotherm determinations in the laboratory. F and k_2 are obtained by fitting models to experimental data. Although relatively simply in representation, first-order rate models are constrained in that the partition coefficient must be derived experimentally or estimated before rate parameters can be fit; also, model parameters have been shown to be dependent on pore water velocity (Brusseau and Rao, 1989; Kookana et al., 1993).

Diffusion Models

More complex diffusion models were also being developed to describe the transfer of solute within the immobile phase. These models differed from the ones previously discussed in that diffusion was considered to be Fickian rather than first-order and the immobile region concentrations are no longer assumed to be uniform.

Fick's second law of diffusion describing the liquid phase concentration distribution in the immobile zone as Equation (10):

$$\frac{\partial C_{im}}{\partial t} = \frac{1}{\delta^\lambda} \frac{\partial}{\partial \delta} (D_a \delta^\lambda \frac{\partial C_{im}}{\partial \delta}) \quad (10)$$

where:

C_{im} = concentration (at path length δ and time t) in the immobile liquid phase

δ = diffusion path length

λ = shape factor

D_a = apparent diffusion coefficient.

The shape is defined by a distribution of capacity along the path length as defined by Equation (11):

$$f(\delta) = \frac{\lambda + 1}{\delta_{\max}^{\lambda-1}} (\delta_{\max} - \delta)^\lambda \quad ; \{0 \leq \delta \leq \delta_{\max}\} \quad (11)$$

Generally Fick's second law of diffusion is shown for a sphere where $\lambda = 2$ and δ_{\max} = the radius of the sphere.

Building on the concepts developed by van Genuchten and Wierenga (1976), Rao et al. (1980a) investigated the use of two-site (bicontinuum) diffusion model to describe

nonequilibrium breakthrough curves. They compared the van Genuchten and Wierenga (1976) model and one incorporating advection, dispersion, and diffusion into spherical aggregates. While both models gave relatively good predictions of experimental results, better predictions were obtained when the rate of mass transfer was described by diffusion into aggregates. Experimental observations (Rao et al., 1980a; 1982) indicated that most sorption data exhibits a two-stage approach to equilibrium, with a rapid initial rate, which accounts for approximately 20-50% of total sorbed, followed by a much slower rate.

Miller (1984) proposed a physical nonequilibrium model that incorporated film transport and intraparticle diffusion as the source of the nonequilibrium breakthrough. The model by Miller (1984) and used by Miller and Weber (1984) was developed using mass transfer and mass balance concepts. The dual resistance model was developed to describe sorption as a series of mass transfer steps involving molecular diffusion through a film layer outside the particle followed by diffusion into the particle itself. The soil phase concentration of solute is described to vary with time as a function of the radial dimension.

Crittenden et al. (1986) developed a Fickian physical nonequilibrium model similar to that of Miller (1984). Their model was based on the presence of aggregates in the soil that caused the nonequilibrium breakthrough curves. This model, the dispersed flow, pore, and surface diffusion model (DFPSDM), included intraparticle diffusion both in the pore space and along the pore surfaces. The DFPSDM included constant advective flow, axial dispersion and diffusion, film mass transfer resistance from the mobile to the immobile phase, local equilibrium between solute adsorbed onto the soil matrix and solute in the intra-aggregate stagnant fluid, and surface and pore diffusion as intra-stationary

phase mass transport mechanisms. As with previous models, the soil column was idealized as containing mobile water and stationary, uniform, spherical aggregates. In addition to the DFPSDM model, Crittenden et al. (1986) present and solve several simplified versions.

Researchers (Goltz, 1986; Wu and Gschwend, 1986; Ball and Roberts, 1991b; Young and Ball, 1995) have applied Fick's second law of diffusion (Equation (9)) where the mechanism for diffusion was in the sorbed phase as well as diffusion in the water filled pores. The models assume linear, reversible equilibrium sorption within the spherical immobile geometry. Although these models allowed good predictive capabilities for the laboratory column studies relative to the various assumptions, substantive knowledge of the particle geometry is necessary to invoke the models.

New Multisite Models

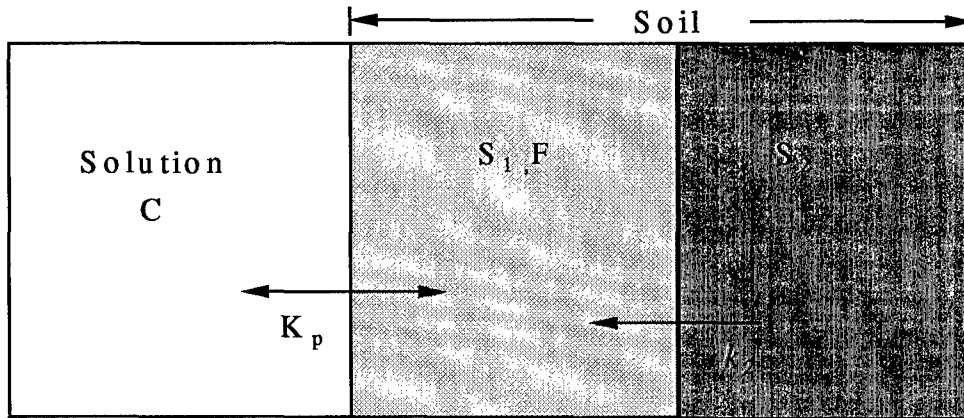
A review of various diffusion and first-order approximations of the diffusion models to date indicates that existing two-site sorption models are deficient in that the model parameters are dependent on pore water velocity (Brusseau and Rao, 1989; Kookana et al., 1993), the models fail to reproduce long-term slow desorption (Karickhoff and Morris, 1985; Connaughton et al., 1993), and existing models based on diffusion assume grain geometries in the absence of physical characterizations. Thus, Heyse (1994) proposed two new multisite models that incorporate more realistic grain geometries. The models are the multiple sites in series (MSS) and multiple sites in parallel (MSP) models. The models build on the concept introduced by Connaughton et al. (1993) that sorption sites are a continuum of compartments, each defined by a first-order mass transfer rate.

The models both assume that sorption can be described as a partitioning process and the rate limiting step is mass transfer by diffusion into either an organic phase or in intraparticle micropores (Chiou et al., 1979, 1983; Brusseau and Rao, 1989; Ball and Roberts, 1991b, Young and Ball, 1995). Where the two-site model uses an average rate constant to define the sizes of sorption site compartments, the MSP uses a frequency distribution for the mass transfer rates as was used by Connaughton et al. (1993). The MSP model is based on the assumption that the diffusion path between the bulk aqueous phase and each sorption site is independent of the diffusion path to all other sites. The advantages of the MSP model are that it is relatively simple computationally, it allows variations in SOM geometry by invoking a stochastic approach, and the number of fitting parameters is limited. The disadvantage in the MSP model lies in the assumption that all concentration gradients are linear.

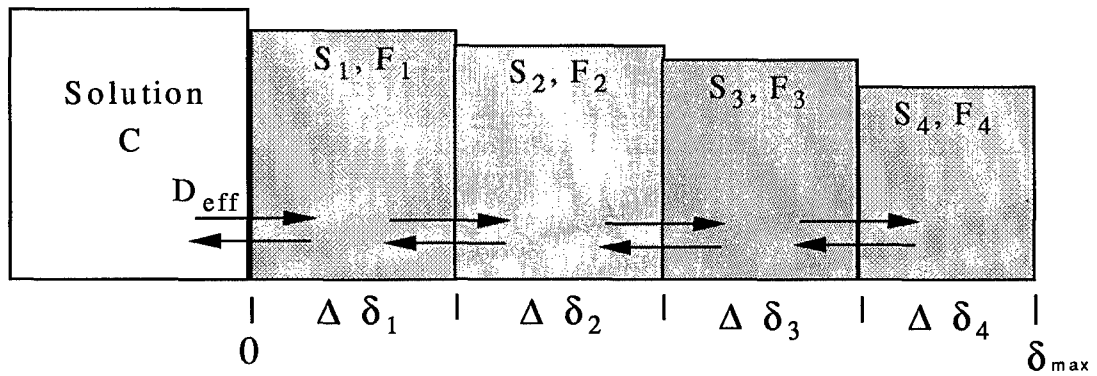
The MSS model describes diffusion through a sequence of compartments using a frequency of sorption capacity along a diffusion path (δ) to define the size of the sorption compartments. The advantage of the MSS model is that while the concentration gradient between each adjacent compartment is linear, the concentration gradient over the entire diffusion path length can be nonlinear (e.g. finite difference approach to diffusion). Like the MSP, the MSS model requires only a limited number of fitting parameters. The disadvantage of the MSS model is it is computationally complex and an average particle is assumed - although the geometry is not limited to a sphere. This research effort seeks to investigate the validity of the MSS model, while the MSP model will be investigated under future efforts.

The MSS model should better describe the diffusion process into uniformly sized films, spheres, or micropores by improved accounting of the abundance of sites at the soil/water interface and deep sites in the soil particle. Based on the approximately shape of soil grains, many models have assumed a spherical, uniformly sized aggregate structure (van Genuchten and Wierenga, 1976; Rao et al., 1980a and b; Nkedi-Kizza et al., 1989; Crittenden et al., 1986; Parker and Valocchi, 1986; Ball and Roberts, 1991b; Rounds et al., 1993; Young and Ball, 1995). The spherical distribution may not adequately account for the abundance of sorption sites at the water/sorbent interface nor the existence of sorption sites at long path lengths. The spherical model is inaccurate in part because real soil consists of a variety of distributions (e.g. films layers, cylinders, spheres and micropores). The effectiveness of the MSS model lies in its potential ability to better depict real average soil distribution of sorption sites. In real soil the distribution of sorption sites is unknown because the soil characteristics (shape factor and diffusion path length) and the effective diffusion coefficients are unknown. The MSS model overcomes these unknowns by using a soil sorption characteristic that is readily assumed, and fitting the remaining soil parameters. For example, the free liquid diffusivity of the solute in the solvent of interest could be used in place of the unknown, variable effective diffusion coefficient. The model would use the free liquid diffusivity and fit the effective shape factor and diffusion path length for an average "virtual" soil particle.

A conceptual MSS model is depicted along with the conventional two-site model in Figure (1).



Conventional Two-site Model



MSS Model

Figure 1. Two-site and MSS mass transfer models. (Heyse, 1994)

The two-site model was described by Equations (7) - (9). The governing equation for a batch system is given by Equation (12):

$$V_l \frac{\partial C}{\partial t} + M_s \frac{\partial S}{\partial t} = 0 \quad (12)$$

where:

$V_l =$ volume of the liquid, and

$M_s =$ mass of the solid.

The concentration in the sorbed phase is normalized to the total mass of sorbent.

The rate of change of sorbed concentration in each compartment of the MSS model is described by Equations (13a) - Equations (13c). If $j = 1$:

$$\frac{dS_j}{dt} = -\frac{D_{eff} F_j}{0.5 \Delta \delta_j} \left[\frac{S_j}{F_j} - K_p C \right] - \frac{D_{eff} F_{j+1}}{\Delta \delta_{j+1}} \left[\frac{\frac{S_j}{F_j} - \frac{S_{j+1}}{F_{j+1}}}{0.5(\Delta \delta_j + \Delta \delta_{j+1})} \right] \quad (13a)$$

If $1 < j < N$:

$$\frac{dS_j}{dt} = -\frac{D_{eff} F_j}{\Delta \delta_j} \left[\frac{\frac{S_j}{F_j} - \frac{S_{j-1}}{F_{j-1}}}{0.5(\Delta \delta_j + \Delta \delta_{j-1})} \right] - \frac{D_{eff} F_{j+1}}{\Delta \delta_{j+1}} \left[\frac{\frac{S_j}{F_j} - \frac{S_{j+1}}{F_{j+1}}}{0.5(\Delta \delta_j + \Delta \delta_{j+1})} \right] \quad (13b)$$

If $J = N$:

$$\frac{dS_j}{dt} = -\frac{D_{eff} F_j}{\Delta \delta_j} \left[\frac{\frac{S_j}{F_j} - \frac{S_{j-1}}{F_{j-1}}}{0.5(\Delta \delta_j + \Delta \delta_{j-1})} \right] \quad (13c)$$

The fraction of sorption sites (F_j) is defined by frequency distribution $f(\delta)$ (Equation (14)):

$$F_j = \int_{\sum_{j-1}^{\Delta\delta_j}}^{\sum_j^{\Delta\delta_j}} f(\delta) d\delta \quad (14)$$

where the frequency distribution of diffusion path lengths is defined by Equation (11).

The size of all compartments sums to unity (Equation (15)):

$$\sum_{j=1}^N F_j = 1 \quad (15)$$

and the sorbed concentration (S) is the sum of the sorbed concentration in each compartment (Equation (16)):

$$\sum_{j=1}^N S_j = S \quad (16)$$

An advantage of the MSS model is the ability to describe diffusion in nonspherical shapes by fitting the λ shape factor parameter. This distribution can describe uniform coatings ($\lambda=0$), cylinders ($\lambda=1$), spheres ($\lambda=2$), higher order geometries ($\lambda > 2$), as well as any combinations of geometries ($\lambda = \text{any real number greater than zero}$). Distributions are defined by only two parameters (δ_{max} and λ).

Batch sorption experiments were used to generate data to determine whether the MSS sorption mass transfer model can correctly predict the known geometry of the nylon balls, paraffin balls and porous ceramic spheres sorbent material. An analytical solution to the diffusion into various geometries in a batch system as a function of time (Crank, 1975) was used to confirm the accuracy of the numerical solution from the MSS model.

Sorption Studies Involving Synthetic Media:

Natural soils vary in type and composition of mineral and organic fraction making them less desirable for use in validating mass transfer models. Researchers have used synthetic media of known and controlled compositions to analyze mass transfer under conditions of greater simplicity than investigations in soil of unknown characteristics. Selection of a surrogate for SOM is challenging because of the heterogeneous nature of SOM in situ, and the choice of media depends on the sorption process of interest: investigations in pore diffusion or polymer-like diffusion.

Although the diffusion of molecules in the polymer-like SOM is still under investigation, much is known about the diffusion in polymers (Crank and Park, 1968). Therefore, researchers have used synthetic organic polymer surrogates in investigating rate limiting behavior with diffusion models. Woodburn et al. (1989) used bonded phase packing materials of chain length C-2-C-8, which is commonly used in reverse-phase liquid chromatography, to investigate the thermodynamics and mechanisms of HOC sorption to these materials. Other researchers have used polyacrylamide gel-exclusion chromatography beads of saturated sizes of 75 to 150 micrometers in diameter to determine the effects of diffusion of ^{14}C -labeled phenol, *p*-nitrophenol and glutamic acid on the kinetics of biodegradation (Scow and Alexander, 1992; Scow and Hutson, 1992). Rebhun et al. (1992) investigated the role of mineral surface adsorption through use of a synthetic aggregate coated with humic acid at varying, but known, amounts. Carroll et al., (1994) investigated the desorption of polychlorinated biphenyls (PCB) from Hudson River

sediments using XAD-4, a high BET surface area polystyrene resin bead, as a PCB adsorbent. The precursor to this work examined spheres of nylon 66 of diameter 0.238, 0.318, 0.476, 0.635, 0.794 cm and similarly sized paraffin beads to measure mass transfer parameters of the sorptive diffusion of HOCs into these polymeric materials and to develop simulation models that describe their behavior (Heyse, 1994). Recently in analyzing sorption as a partitioning process combined with the occurrence of adsorption, Xing et al. (1996) used rubbery hydrophobic and hydrophilic polymers and a glassy polymer as model sorbent materials. They also used a mesoporous amorphous silica as a model for hydroxylated mineral silica.

Likewise researchers have used surrogate media to investigate pore diffusion as a cause of rate limiting mass transfer. Rao et al. (1980b) used porous ceramic spheres made of fired kaolinite clay, an aluminosilicate mineral of formula $\text{Al}_2(\text{OH})_4\text{Si}_2\text{O}_5$, of size 0.55 and 0.75 cm in radius. They measured mass transfer parameters for the nonadsorbed solutes $^3\text{H}_2\text{O}$ and $^{36}\text{Cl}^-$ and used the parameters in the development of diffusion simulation models. Scow and Alexander (1992) and Scow and Hutson (1992) used the porous spheres courtesy of Rao et al. (1980b) in addition to the polyacrylamide gel-exclusion chromatography beads discussed above to determine the effects of pore diffusion of ^{14}C -labeled phenol, *p*-nitrophenol and glutamic acid on the kinetics of biodegradation. In a study to investigate the effects of pore size, particle size and lack of microporosity, Farrell and Reinhard (1994) used silica gels, glass beads and clay montmorillonite to analyze TCE desorption. The differing media allowed targeted investigations into desorption phenomena of meso-, micro- and nonporous solids.

The use of synthetic media gives researchers more control to investigate sorption properties on media of known characteristics including diffusion coefficients, distribution characteristics and geometry. Data gained from studies on synthetic media improve the researcher's ability to interpret investigations with real soil.

III. Methodology

Materials:

Solid Phases

The sorbent materials in this study were chosen to allow investigation of diffusive transport. The synthetic polymers were chosen for their ability to substitute for modeling mass transfer rate limitations of SOM and for their differing, but known, sorption coefficients, diffusion coefficients, and geometries. The materials include paraffin wax (Aldrich Chemical Co., CAS registry # 8002-74-2), nylon 66 spheres of sizes 0.238, 0.318, 0.476, 0.635, 0.794 cm diameter (Small Parts Inc.), and porous ceramic spheres made of fired kaolinite clay, an aluminosilicate mineral of formula $\text{Al}_2(\text{OH})_4\text{Si}_2\text{O}_5$, of sizes 0.55 and 0.75 cm in radius (Rao et al., 1980b).

Paraffin wax spheres were prepared from paraffin chunks as follows. A small quantity of paraffin was placed in a beaker and heated just to melting. The liquid paraffin was then poured into a small plastic mold which upon solidification and removal formed small paraffin plugs. The plugs were then formed into spheres by pressing and turning a paraffin plug through a 0.483 cm diameter hole in a stainless steel template. This was completed multiple times until a uniform paraffin sphere of 0.476 cm diameter was formed.

Solute

Anthracene (99%, Aldrich Chemical Co., CAS # 120-12-7), a component of petroleum fuels and coal tar, is an polyaromatic hydrocarbon of molecular weight 178.2

g/mol. Anthracene has good adsorption at 254 nm and is easily analyzed with HPLC ultraviolet detection. The compound is stable, nonpolar, and of low volatility making it ideal for laboratory sorption studies.

Liquid Phases

The liquid phases of all experiments consisted of a 1:1 (v/v) solution of methanol (99.9 + %, Aldrich Chemical Co., CAS # 67-56-1) and distilled water (Aldrich Chemical Co., CAS # 7732-18-5) with differing concentrations of anthracene (≤ 0.9 mg/L). The 1:1 methanol and water ratio was chosen to reduce sorption by vial glass and Teflon covered septa and to accelerate the sorptive process under laboratory conditions. To protect anthracene from photodegradation all liquid phases were stored in amber glassware.

Experiments:

Isotherm

Nylon was prepared by independently crushing nylon spheres of diameter 0.794 and 0.318 cm by first placing them in a flask of liquid nitrogen. Once frozen, the spheres were removed and placed between a durable cloth and crushed with a hammer on a hard surface. Four initial concentrations of the liquid phase were used; 0.81, 0.61, 0.41, and 0.20 mg/L of anthracene. For each size of nylon sphere, approximately 0.07 grams of its crushed form was weighed and placed into 4 mL amber vials. Each concentration of stock solution was added to each type of crushed nylon sphere, 0.794 and 0.318 cm, with one duplicate each. In addition four vials were filled with each concentration of stock solution for the quantitative determination of the initial concentration of these solutions. Two vials containing 0.07 grams of crushed nylon of each size were filled with analyte free 1:1 liquid phase to act as blanks. Isotherm experiment set up data is included in Appendix B. The vials were agitated continuously on a shaker table to ensure that bulk liquid was completely mixed. The solutions have not reached equilibrium to date.

Rate Studies

The rate of sorption was measured using different types, sizes, and combinations of the solid phases. All experiments were performed in batch by placing the solid phase and anthracene containing liquid phase in Teflon capped amber vials or bottles. The containers were agitated and sampled periodically to monitor the change in liquid phase anthracene concentration using HPLC as the batch system reached equilibrium. Blanks

consisting of anthracene free liquid phase and solid phase were used to ensure that there was no interference associated with the solid phase.

Nylon 66

Batch sorption rates were measured for five sizes of nylon spheres; 0.238, 0.318, 0.476, 0.635, 0.794 cm diameter spheres as well as for a mixture of all five sizes. Nylon spheres were weighed to be as close to 0.57 grams as possible and placed in 40 mL amber vials, with the number of balls weighed noted. Each size nylon sphere including the mixed sizes was run in triplicate. To each vial, approximately 40 mL of 0.81 mg/L anthracene liquid phase was added then weighed using an analytical balance. In addition, two blanks were made consisting of mixed sizes of nylon spheres with analyte free 1:1 liquid phase. Three 4 mL vials were filled with the 0.81 mg/L anthracene liquid phase to determine quantitatively the concentration of the initial condition and to act as a laboratory control. A summary of nylon 66 experimental conditions is included in Appendix B.

For each type of solid phase, two of the three vials were sampled approximately every ten days by extracting not more than one milliliter of the liquid phase and analyzing by HPLC. Vials were weighed after sampling to determine mass of removed liquid phase. As a control, the third vial remained unsampled until it was determined equilibrium was reached. In addition, the initial condition vials were sampled repeatedly over the course of the experiment to investigate possible loss of anthracene mass due to volatilization, degradation, and/or sorption on vial glass and septa.

Porous Ceramic Spheres

Batch diffusion rates were independently measured for porous ceramic spheres of 0.55 and 0.75 cm radii. The spheres were placed in a vacuum flask with anthracene free liquid phase and allowed to become saturated under reduced pressure over a 24 hour period. Eight 0.55 cm radii sized spheres that were placed in a 40 mL amber vial with 19 mL of 0.80 mg/L anthracene liquid phase. Six 0.75 cm radii sized spheres were placed in a 250 mL amber bottle with 35 mL of 0.80 mg/L anthracene liquid phase. Both of these systems were prepared in duplicate. A blank consisting of the same conditions as the 0.55 cm sized spheres was placed in another 40 mL amber vial with 19 mL of anthracene free liquid phase. Each vial and bottle were capped with Teflon lined septa and gently agitated by hand periodically. Each container was sampled total duration of about 48 hours by extracting about 1 mL and analyzing by HPLC. Vials were weighed after sampling to determine mass of removed liquid phase. A summary of the porous ceramic sphere (SB and LB, small and large beads respectively) experimental conditions is included in Appendix B.

Mixed Porous Ceramic and Paraffin Spheres

Batch diffusion rates were also measured for a mixture of media, which contained both sizes of ceramic spheres and paraffin spheres of 0.249 cm radius. A duplicate pair of conditions was prepared consisting of six 0.55 and three 0.75 cm radii sized saturated spheres as well as seven paraffin spheres that were placed in 40 mL amber vials with 31 mL of 0.80 mg/L anthracene liquid phase each. In addition, a blank consisting of the same amount and type of solid phase was placed in another 40 mL amber vial but anthracene

free liquid phase was added. Each vial was capped with Teflon lined septa and gently agitated by hand periodically. Each container was sampled for total duration of four weeks by extracting about 1 mL and analyzing by HPLC. Vials were weighed after sampling to determine mass of removed liquid phase. A summary of the mixed paraffin and porous ceramic sphere (PMB) experimental conditions is included in Appendix B.

Analytical Methods

Quantitative determinations were accomplished using a Hewlett Packard 1090L, High Performance Liquid Chromatograph (HPLC). The operating conditions consisted of a 100 microliter sample size, 100% methanol as mobile phase, mobile phase velocity of 0.4 mL/min, and oven temperature of 32 degrees Celsius. Separations were accomplished using a 150 x 4.6 mm Alltech, Adsorbosphere analytical column, with a C18 bonded phase, and 5 micron packing. Detection was accomplished using a filter photometric detector set at 254 nm. The instrument was calibrated using a series of standards of different concentration. The standard stock solution was made by weighing a known amount of anthracene in a 100 mL class A volumetric flask and diluting to the mark with methanol. A series of standards of varying concentrations was made by diluting the standard stock solution with methanol using class A pipets. Instrumental controls were performed prior to analyzing experimental samples and again after every ten experimental samples to verify instrument integrity.

IV. Data Analysis and Model Simulation

Experimental Data Analysis:

Mass balance was used to determine sorbed phase concentrations of the solid phase for each experiment. The loss of anthracene mass due to volatilization, degradation, and/or sorption on vial glass and septa was assumed to be negligible but was quantified using data obtained from the blanks and controls.

Nylon 66 Sphere Rate Study

Because each vial was sampled repeatedly by removing a small aliquot for analysis, the boundary conditions changed following each sampling event. To account for the loss of mass from sampling, the following relation (Equation (17)) was used in determining the solid phase concentration:

$$C_{s(n)} = \frac{C_{l(i)}V_{l(i)} - I \sum_{j=1}^n C_{l(j)}(V_{l(j-1)} - V_{l(j)}) - C_{l(n)}V_{l(n)}}{M_s} \quad (17)$$

Experimental data was plotted as C_s/C_l versus time in days as seen in Figure (2). When C_s is calculated on a partitioning basis (Equation (17)), the value of C_s/C_l should eventually approach the equilibrium K_p if the sorption mechanism is partitioning. For a system involving the same solute and sorbent, C_s/C_l should eventually approach the same equilibrium K_p . At 120 days into the experiment it is obvious that either the media is not at equilibrium, or the sorption mechanism is not partitioning if it is at or near equilibrium.

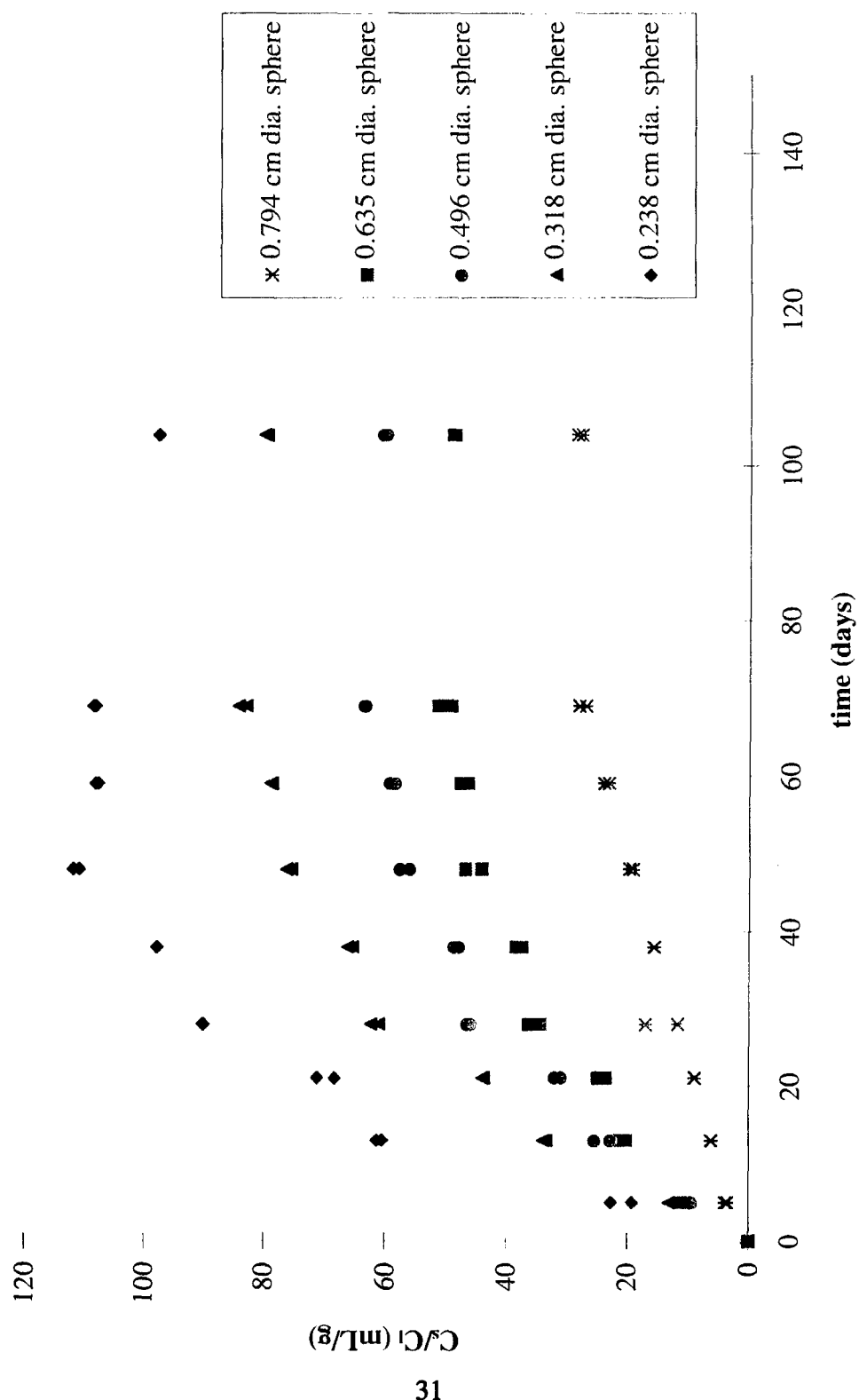


Figure 2. Uptake of Anthracene by Nylon 66 (partitioning basis).

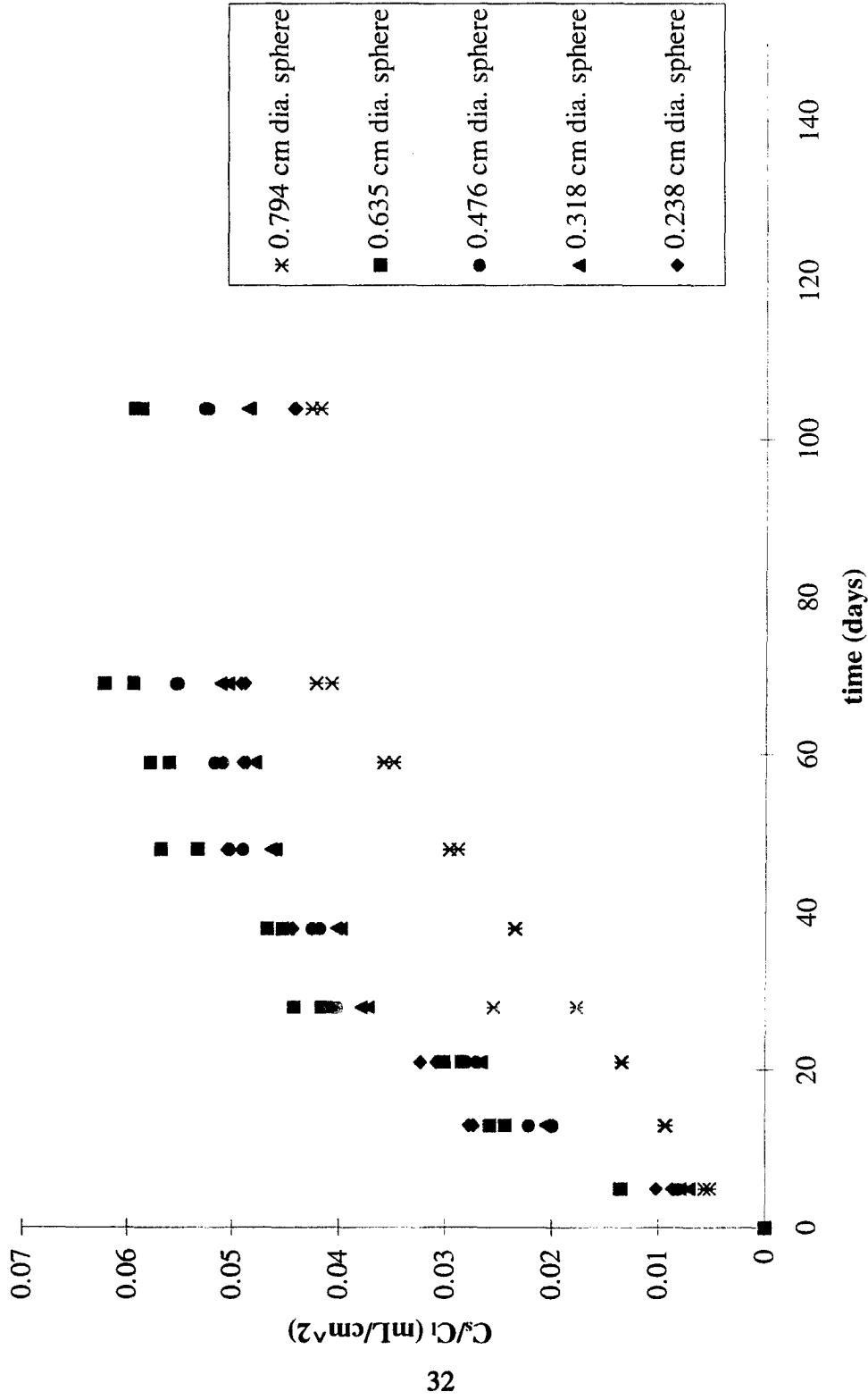


Figure 3. Uptake of Anthracene by Nylon 66 (adsorption basis).

Conversely, when C_s is calculated per surface area of the solid phase, plotting the value of C_s/C_l over time would approach an adsorption coefficient, K_{ad} , if the sorption mechanism is adsorption. Calculating C_s per surface area solid phase (Equation (18)):

$$C_{s(n)} = \frac{C_{l(i)}V_{l(i)} - \left[\sum_{j=1}^n C_{l(j)}(V_{l(j-1)} - V_{l(j)}) \right] - C_{l(n)}V_{l(n)}}{SA_s} \quad (18)$$

The uptake data is presented on an adsorption basis in Figure (3). The data are grouped closer together than in Figure (2). This may indicate that sorption of anthracene by nylon 66 is an adsorption process. It could also mean that sorption of anthracene by nylon 66 is a very slow partitioning process, since the early stages of partitioning would look similar to adsorption.

Figure (4) represents paraffin rate data from deVenoge (1996) that is plotted as C_s/C_l versus time in days with C_s calculated on a partitioning basis as defined in Equation (17). As expected for partitioning media, the value of C_s/C_l for the paraffin over time approached the same equilibrium K_p for all sphere sizes. When the paraffin data are plotted on an adsorption basis, all sphere sizes do not approach the same equilibrium K_{ad} (Figure (5)). These data clearly demonstrate that the sorption mechanism for anthracene by paraffin is partitioning.

An argument in favor of sorption of anthracene by nylon 66 by partitioning can be made by examining the apparent rate at which the anthracene is sorbed by sphere size. If the sorption mechanism was on an adsorption basis, the larger spheres would have the fastest uptake. Figure (3) clearly shows the largest spheres to have the slowest uptake.

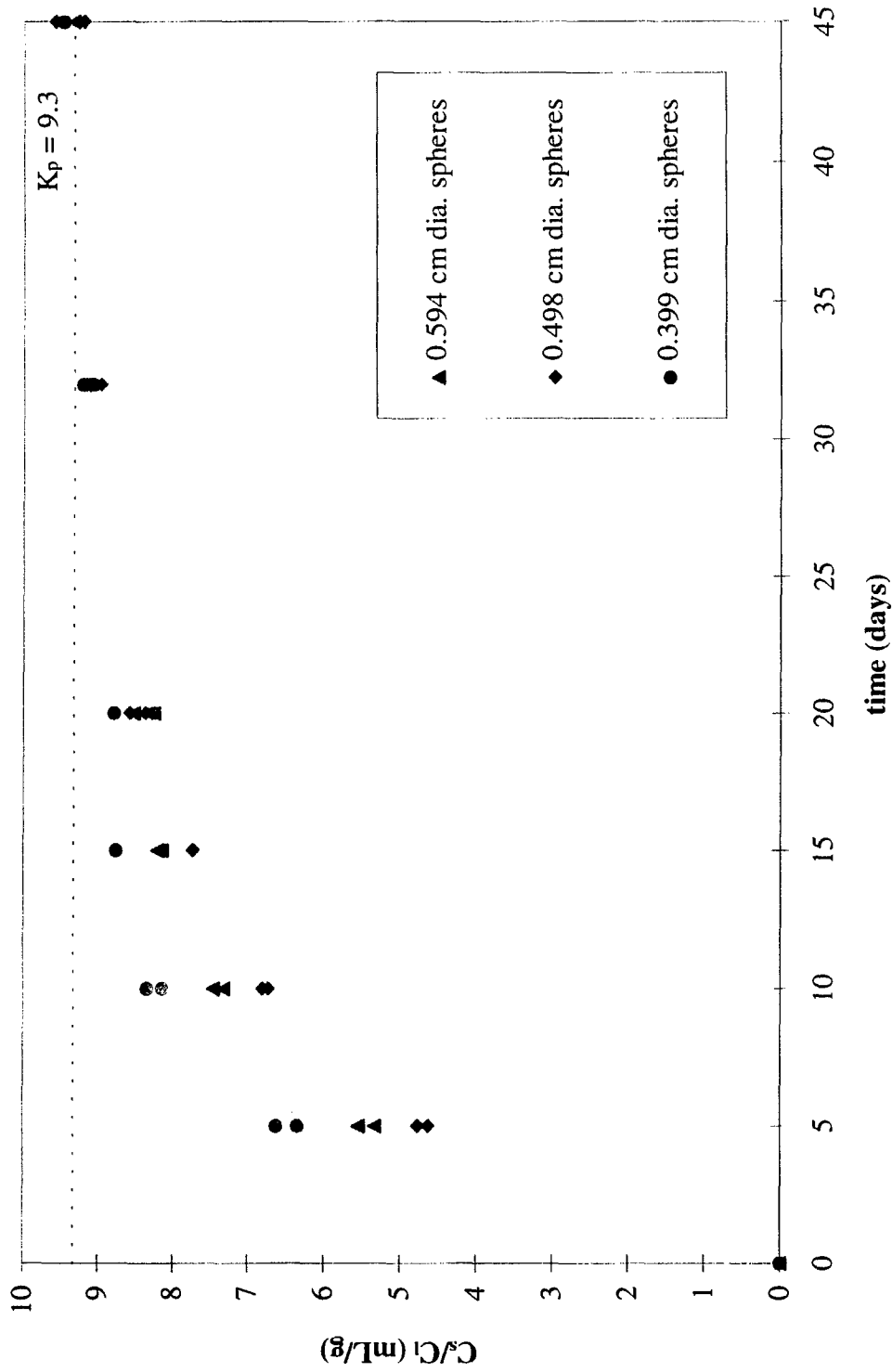


Figure 4. Uptake of Anthracene by Paraffin (partitioning basis).

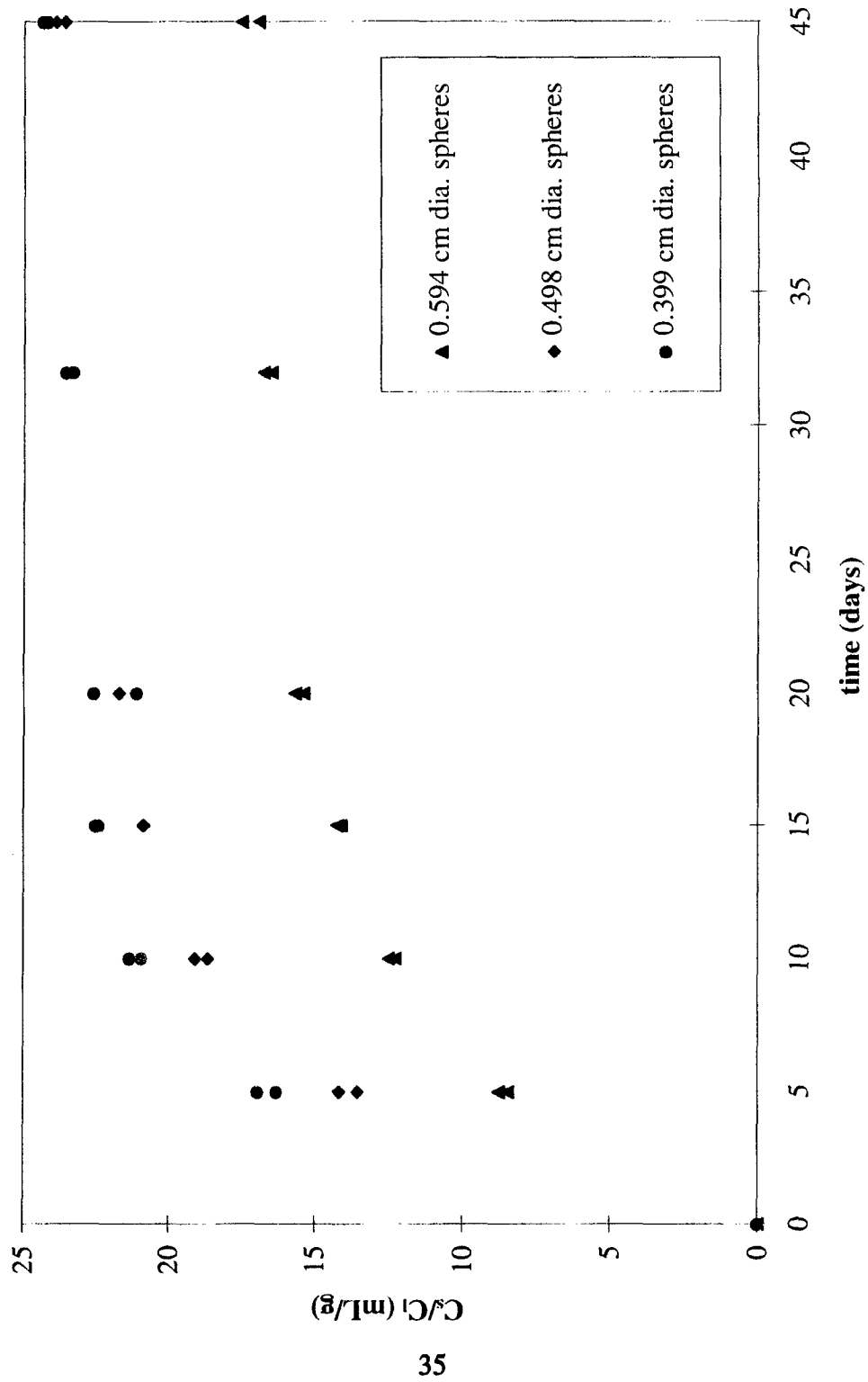


Figure 5. Uptake of Anthracene by Paraffin (adsorption basis).

The data for anthracene uptake by paraffin on an adsorption basis (Figure (5)) show the largest paraffin spheres to have the slowest uptake. This is as expected since anthracene uptake by paraffin is not on an adsorption basis. Similarly, because the data represented in Figure (3) also show the largest nylon 66 spheres to have the slowest uptake, anthracene uptake by nylon 66 may not be on an adsorption basis.

Since the sorption mechanism for anthracene by nylon 66 could not be defined with certainty, it was not appropriate to fit partitioning parameters to the data.

Ceramic Sphere Rate Study

Solid phase concentrations of the porous ceramic spheres were calculated using Equation (19):

$$C_{s(n)} = \frac{C_{l(i)}V_{l(i)} - \left[\sum_{j=1}^n C_{l(j)}(V_{l(j-1)} - V_{l(j)}) \right] - C_{l(n)}V_{l(n)}}{V_s} \quad (19)$$

where:

$V_s =$ bulk volume of ceramic sphere.

Experimental data was plotted as (C_s/C_1) versus time in hours as seen in Figure (6).

Ceramic and Paraffin Sphere Rate Study

Solid phase concentrations of the ceramic and paraffin spheres were calculated using (Equation (20)):

$$C_{s(n)} = \frac{C_{l(i)}V_{l(i)} - \left[\sum_{j=1}^n C_{l(j)}(V_{l(j-1)} - V_{l(j)}) \right] - C_{l(n)}V_{l(n)}}{V_s + M_s} \quad (20)$$

Experimental data was plotted as (C_s/C_1) versus time in days as seen in Figure (7).

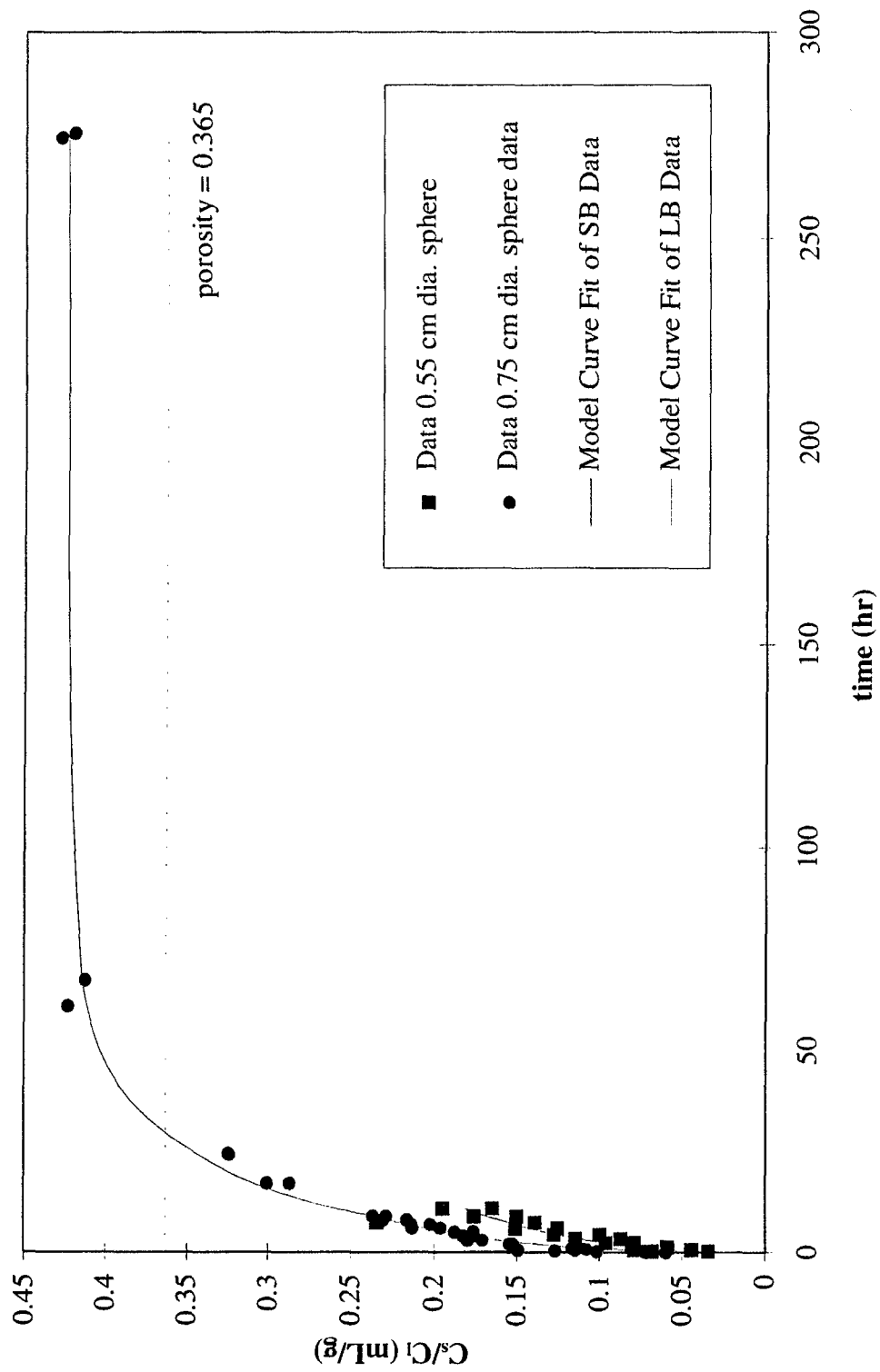


Figure 6. Uptake of Anthracene by Ceramic Porous Spheres.

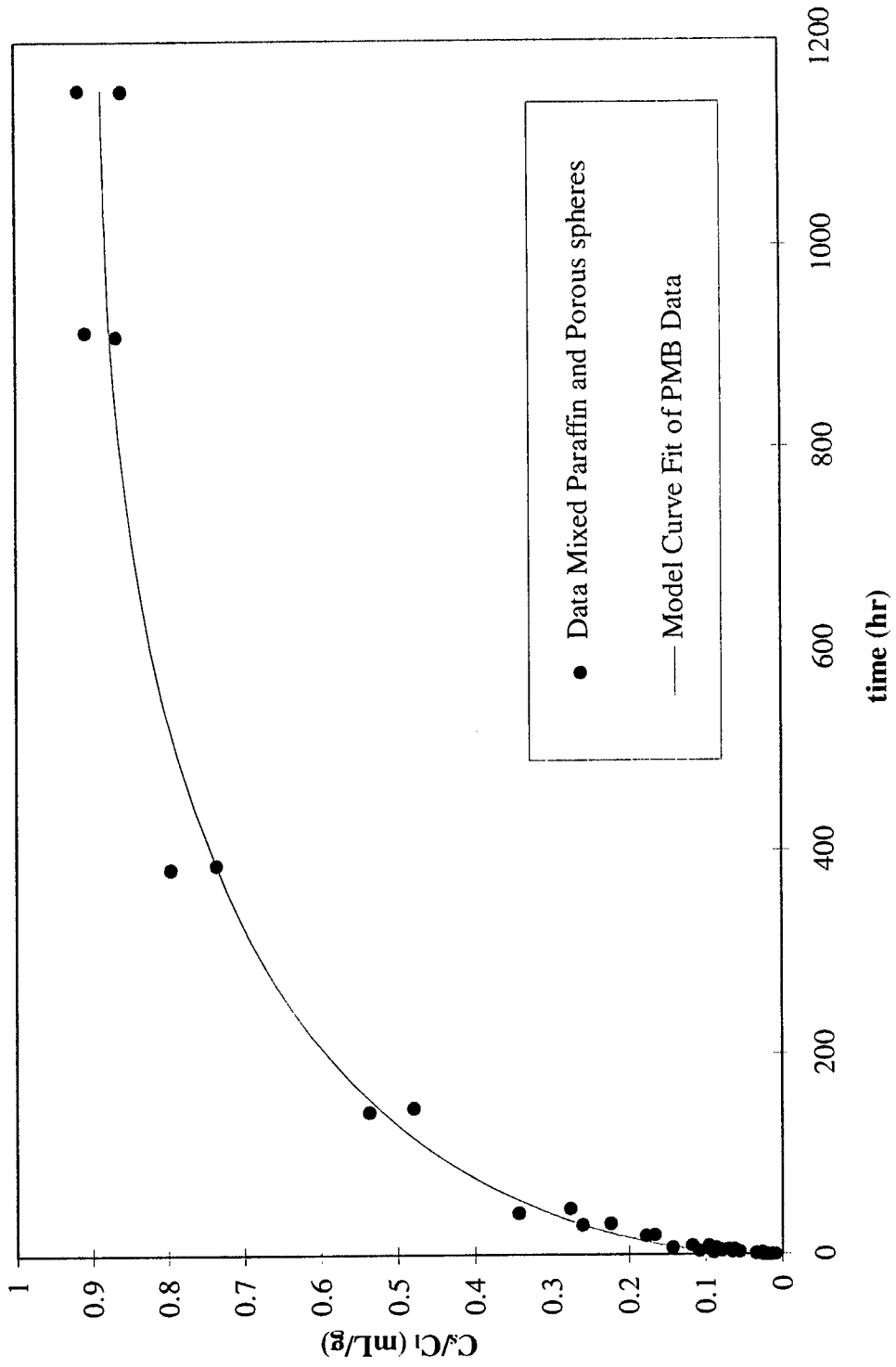


Figure 7. Uptake of Anthracene by Ceramic and Paraffin Spheres.

The expected final equilibrium $C_{s(f)}/C_{l(f)}$ for the porous ceramic sphere rate study was the porosity of $\eta = 0.365$. Instead, the ratio of the concentrations approached a value greater than the capacity of the porosity (Figure (6)). To account for this difference anthracene must not only be diffusing into the micropores but may also be adsorbing to the silanol groups (SiOH) of the kaolinite mineral structure. This behavior is well documented and has been measured for substituted aromatic compounds on kaolinite (Schwarzenbach and Westall, 1981). If the process for this unexpected sorption is adsorption, additional steps to prevent the adsorption from occurring can be incorporated into future experimental procedures. The silanol groups of the porous ceramic spheres can be deactivated by silanization with dimethylchlorosilane (DMCS) followed by a methanol rinse. This reaction replaces the silanol hydrogen with dimethylmethoxysilane [$\text{SiOSi}(\text{CH}_3)_2\text{OCH}_3$] which minimizes adsorption by solute species. Conversely, one may assume that the additional sorption is linear, reversible, and fast relative to the slow, diffusive transport in the micropores and no procedural adjustments are necessary. These assumptions were made and the increased sorption was included in the MSS model simulations.

Blanks and Controls

Instrumental controls were analyzed repeatedly over the course of experimental analysis. Controls were performed before experimental samples were analyzed and again after analysis of every ten experimental samples. The experiments that were analyzed over the course of many weeks, such as the nylon 66 sphere rate study and the mixed ceramic and paraffin sphere rate study, included many controls. The ceramic sphere rate studies

were conducted over the course of hours and therefore do not include many controls. With the exception of a few outliers, instrument controls fall within a 95% confidence interval.

An initial condition vial was sampled repeatedly over the course of the nylon 66 sphere rate study to determine the effects of loss of anthracene due to volatilization, degradation, and/or sorption on vial glass and septa. After 69 days a loss of less than 2% was found. Significant volatilization of anthracene is unlikely as is degradation in the methanol/water solution. Also, the anthracene would not preferentially sorb to the glass from the liquid 50-/50 (v/v) methanol/water phase. Loss due to sorption by the Teflon septa is possible, yet improbable. The amorphous septa would possibly swell during exposure to the liquid phase enhancing sorptive processes as in IOMD (Lion et al., 1990). However, during the experiment the vials were placed upright on a shaker table and rarely inverted. Solvent contact with the septa was minimal and not of length to induce septa swell and subsequent sorption. The loss is most probably due to operator error in the experiment or error in instrument analysis.

Blanks containing the solid phase of study and anthracene free liquid phase were made for all experiments. In all cases no trace of anthracene was detected in the blanks.

Model Simulation and Validation:

With the data from the batch sorption experiments, the MSS sorption mass transfer model was used to estimate the effective diffusion rate coefficient for anthracene in the porous ceramic sphere and mixtures of porous ceramic and paraffin. The numerical code for the MSS model written in FORTRAN (Appendix C) minimizes the weighted sum of square for error residuals (SSQ) for the uptake of solute by using the liquid phase concentration (Equation (19)) and time sampled. Mass transfer parameters were estimated from breakthrough curve data by performing multiple nonlinear least squares regressions minimizing SSQ solving for the parameters that best fit the rate data (Meeter and Wolfe, 1968). The model converts the continuous frequency distribution of sorption sites within the volume of the sphere (Equation (11)) into a discrete distribution. Using synthetic media, the model will optimally converge on the known geometric parameters (maximum diffusion path length and shape factor). The MSS numerical solution was verified using an analytical solution (Crank, 1975).

The MSS model was used to estimate the effective diffusion coefficients for the homogeneous experiments involving porous ceramic spheres. The model estimated the effective diffusion coefficients using the known maximum diffusion path length, δ_{max} , and shape factor, λ , for the porous ceramic spheres and an average K_p found in independent experiments with the porous ceramic spheres. The fitted diffusion coefficients and SSQ are shown in Table 5.

Table 5. Fit D_{eff} using known δ_{max} and λ .

Solid Phase	K_p	D_{eff} (fit) (cm ² /sec)	Std Dev	δ_{max} (cm)	λ	SSQ
0.55 cm dia. (vial 1)	0.425	1.21E-07	8.80E-09	0.55	2	1.26E-03
0.55 cm dia. (vial 2)	0.425	2.25E-07	3.45E-08	0.55	2	1.40E-02
Combined 0.55 cm dia.	0.425	1.65E-07	1.20E-08	0.55	2	1.67E-02
0.75 cm dia. (vial 1)	0.425	8.99E-07	4.58E-08	0.75	2	3.24E-03
0.75 cm dia. (vial 2)	0.425	9.29E-07	8.71E-08	0.75	2	1.05E-02
Combined 0.75 cm dia.	0.425	9.19E-07	4.82E-08	0.75	2	1.35E-02

Considering the model results (Table (5)) and contrary to that anticipated, it appears that diffusion in the smaller spheres (0.55 cm dia.) is occurring at a faster rate than for the larger spheres (0.75 cm dia). This is possibly an artifact of the incomplete experiment small sphere experiment as unfortunately the small sphere data did not reach equilibrium before the HPLC suffered mechanical failure. However, using the K_p from the large spheres to fit the D_{eff} should have accounted for the lack of a complete data set and resulted in a similar D_{eff} for the two experiments. It is possible that the K_p for the small spheres is not the same as the K_p for the large spheres although unlikely. A more probable reason for the difference in D_{eff} is in the experimental conditions. Preliminary experimental runs with the solute and sorbent using shaker tables to establish well-mixed conditions resulted in a cloudy liquid phase that clogged HPLC tubing and filters. Subsequent runs

were not agitated, merely swirled. It is possible the difference in D_{eff} between the large and small spheres is due to insufficient mixing.

The results for D_{eff} in the large spheres (0.75 cm dia.) were compared with the fitted diffusion coefficients of previous research using the same size porous ceramic media, $^{36}\text{Cl}^-$ and $^3\text{H}_2\text{O}$ solutes, modeled, however, with a different analytical model (Rao et al., 1980). Before a direct comparison can be made, the D_{eff} for the anthracene (a sorbing solute) was adjusted to account for retardation due to sorption when compared to the nonsorbing solutes used by Rao et al. (1980). This adjustment was made with Equation (21) where the effective diffusion for the sorbing solute is multiplied by the retardation factor, R , for the sorbing solute to give an equivalent effective diffusion as though the solute were nonsorbing.

$$D_{eff(nonsorbing)} = RD_{eff(sorbing)} \quad (21)$$

The diffusion coefficient found in this effort is an order of magnitude smaller (Table 6.) than that found by Rao et al. (1980). This may indicate that diffusive transport in this experiment was somewhat slower than for the work by Rao et al. (1980b), possibly due to the differences in solutes for the experiments.

Table 6. Effective Diffusion Coefficients for Nonsorbing Solutes into 0.75 cm dia. Porous Ceramic Spheres.

Diffusion Coefficient cm ² /hr	Anthracene	$^{36}\text{Cl}^-$	$^3\text{H}_2\text{O}$
D_{eff}	0.0039	0.012	0.012
D_o	0.0316	0.0396	0.0396

The tortuosity, τ , is represented by a ratio of the effective diffusion to the diffusion coefficient for a given media (Equation (22)).

$$\tau = \frac{D_{eff}}{D_o} \quad (22)$$

Investigating the ratio of the effective diffusion to the diffusion coefficient for each experiment respectively results in a τ for this experiment equal to 0.122 and for the work by Rao et al. (1980) equal to 0.303. It would be expected that for the systems using the same sorbent, τ would be equivalent. Although relatively close, the values are not equivalent. One possible reason for the variation may be due to steric hindrance due to the comparatively large size of the anthracene molecules. However, because the size of the "micropores" of the ceramic spheres are presumed large relative to the anthracene molecules, this would be unlikely. Another possible and perhaps more probable reason could be due to experimental technique. In both this experiment and the Rao et al. (1980) experiment the vials were swirled intermittently. Perhaps the swirling techniques employed in this experiment were not sufficient to establish a well-mixed liquid phase, thus impacting diffusive transport.

For real soils, the media shape properties are unknown. Real soil is a heterogeneous mix of particles with differing partitioning coefficients, K_p , effective diffusion, D_{eff} , and distribution of sorption sites, $f(\delta)$. The model must be able to overcome these unknowns by using sorption characteristics that is readily available or assumed, and fitting as few remaining soil parameters as possible. Using an average K_p for the soil and the free liquid diffusivity for the solute of interest, the model can be used to fit

parameters of the average soil particle. This average or virtual particle can be defined by the shape properties of a virtual maximum path length, δ_{max}^* , and some shape factor, λ . Converting the maximum path length is necessary to adjust for model use of the free liquid diffusivity to fit the soil parameters. The real maximum path length, δ_{max} , was converted to a virtual maximum path length, δ_{max}^* , using Equation (23):

$$\delta_{max}^* = \sqrt{\frac{D_o}{D_{eff}}} \delta_{max} \quad (23)$$

D_o is the free liquid diffusivity of anthracene in 50/50 (v/v) methanol/water which was used in place of the unknown effective diffusion coefficient to fit the shape parameters. Table 7 shows the MSS model results using the free liquid diffusivity to fit δ_{max}^* and λ for the heterogeneous system of mixed paraffin and porous ceramic spheres.

Table 7. Two-parameter fit, δ and λ , using free-liquid diffusion coefficient, D_o .

Solid Phase	K_p	D_o (cm ² /sec)	δ_{max}^* (fit) (cm)	Std Dev	λ (fit)	Std Dev	SSQ
PMB 1	0.888	8.37E-06	159.4	25.2	60.1	14.6	1.45E-01
PMB 2	0.888	8.37E-06	87.4	16.8	31.6	7.9	1.39E-02
Combined PMB	0.888	8.37E-06	122.4	16.5	46.5	8.75	4.07E-02

Because the actual media used is of known geometric properties, the true distribution of sorption sites is also known. The graphical representation of the true distribution of sorption sites was developed using a composite of the sorbent geometry for each media in the system; 0.55 cm diameter porous ceramic spheres, 0.75 cm diameter porous spheres and 0.499 cm diameter paraffin spheres. The mass fraction contribution of

each media type were summed to create a resultant combined, true distribution (Figure (8)).

Using a distribution of sorption capacity along the path length as defined by Equation (11), the fitted values of δ_{max}^* and λ were plotted and compared to the true average distribution of sorption sites (Figure (9)). The model fit is not coincident with that of the true distribution for the media except at long path lengths. One possible reason for this is in the computation of the true distribution of sorption capacity sites along the path length. The assumptions entered into in this investigation and deemed necessary for analysis centered on the use of a synthetic media. By using synthetic media it was assumed that soil sorption characteristics and geometric characteristics were known. It is possible that the experiment as conducted was insufficient to establish known soil sorption characteristics. For example, the experiment was unable to be run until equilibrium conditions were reached. Also, as was previously suggested, it is possible that conditions were not sufficient to establish a well-mixed liquid phase. Thus, because the "true" distribution may have been developed with inaccurate data, it cannot be said that the soil sorption characteristics are known. If this is the case, the model has cannot be evaluated as there is no known true distribution of sorption sites. Future experiments to assess the model validity must ensure experimental conditions are such that soil sorption characteristics are accurate so that they may be used to develop a true distribution of sorption sites.

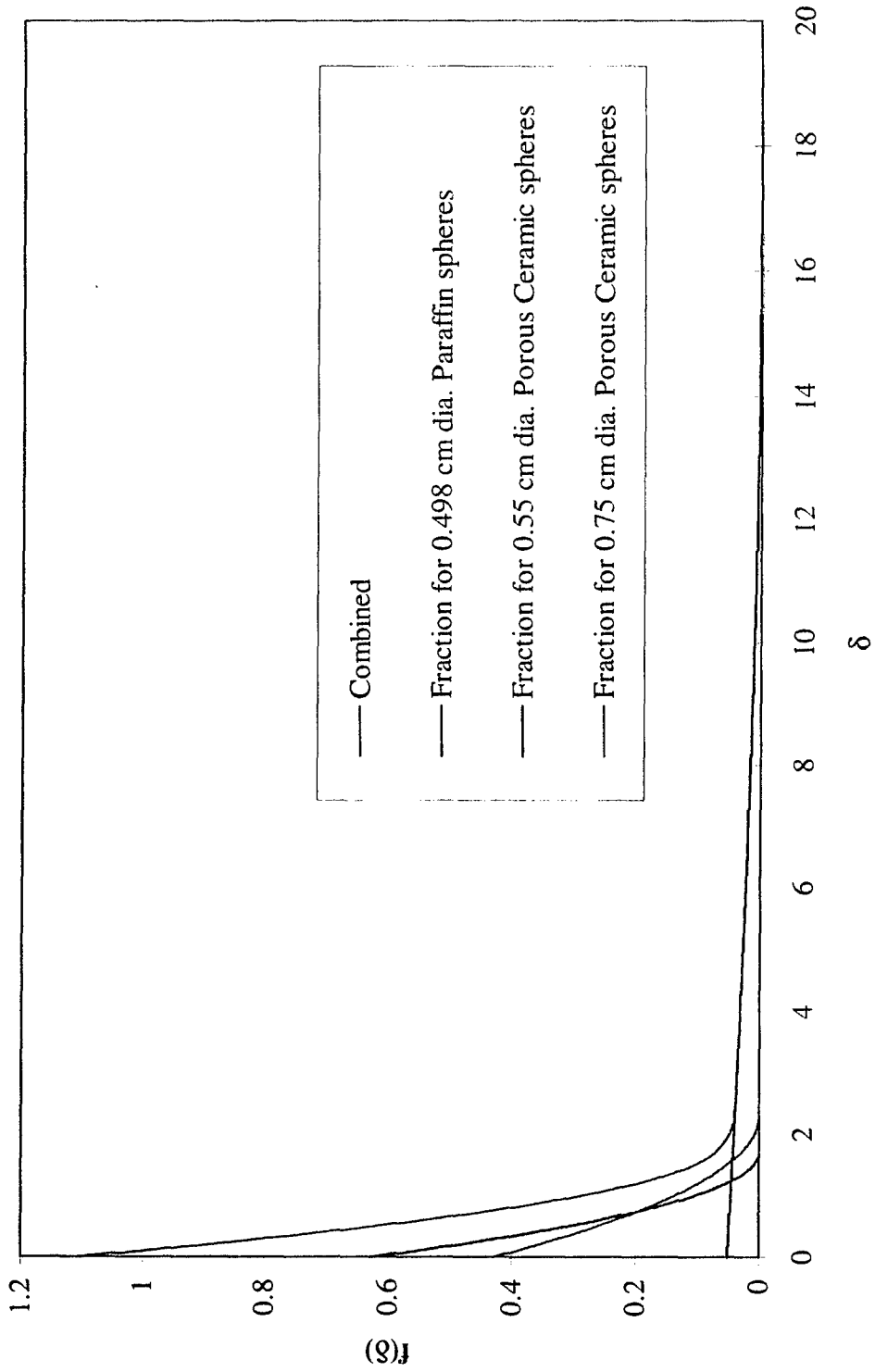


Figure 8. True "Virtual" Geometry created from Composite of Paraffin and Porous Ceramic Spheres.

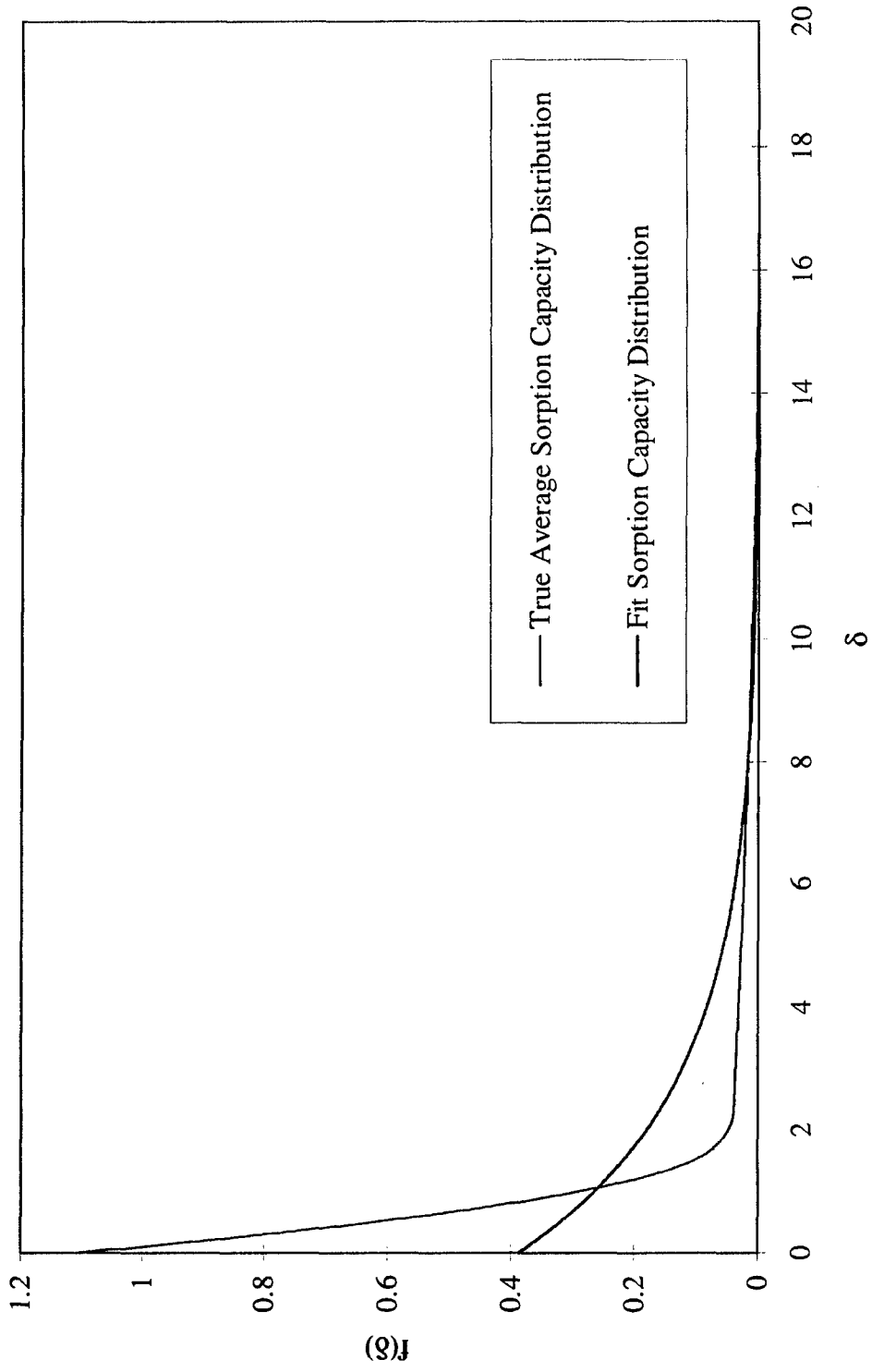


Figure 9. True and Fitted Distributions of Sorption Capacity for Mixed Media Experiment.

V. Summary and Conclusion

The sorption rates of anthracene on synthetic media consisting of nylon 66, porous ceramic, paraffin and mixtures of porous ceramic and paraffin spheres were measured using HPLC. The results were interpreted by use of a multisite diffusion mass transfer model.

The time required to establish equilibrium conditions for the nylon 66 was in excess of the allotted time for this research effort. The low rates of uptake suggest the nylon 66 to be a highly condensed polymer where the time required to reach equilibrium is much greater than for less condensed polymers such as the paraffin.

The rate behavior in the porous ceramic spheres was slower than published results using the same media although this may be attributed to experimental techniques. The rate parameters inferred from the data were not entirely consistent among sizes of spheres, probably attributed to experimental deficiencies where equilibrium conditions were not sampled due to mechanical failure of the analytical instrumentation.

These results demonstrate the significance of adequate experimental conditions to establish accurate depiction of the distribution of sorption sites in the synthetic media to allow model comparison. The experimental results reported here have important implications for the proper design of corresponding laboratory experiments.

VI. References

- Alexander, M., Biodegradation and Bioremediation. San Diego: Academic Press, Inc., 1994.
- Augustijn, D.C.M., Chemodynamics of Complex Waste Mixtures: Applications to Contamination and Remediation of Soils and Aquifer Media, PhD Dissertation, University of Florida, Gainesville FL 1993.
- Ball, W.P. and P.V. Roberts, "Long-Term Sorption of Halogenated Organic Chemicals by Aquifer Material. 1. Equilibrium," Environmental Science and Technology, Vol. 25, pp. 1237-1249, 1991a.
- Ball, W.P. and P.V. Roberts, "Long-Term Sorption of Halogenated Organic Chemicals by Aquifer Material. 2. Intraparticle Diffusion," Environmental Science and Technology, Vol. 25, pp. 1237-1249, 1991b.
- Brusseau, M.L., R.E. Jessup and P.S.C. Rao, "Nonequilibrium Sorption of Organic Chemicals: Elucidation of Rate-Limiting Processes," Environmental Science and Technology, Vol. 25, pp. 134-142, 1991a.
- Brusseau, M.L. and P.S.C. Rao, "The Influence of Sorbate-Organic Matter Interactions On Sorption Nonequilibrium," Chemosphere, Vol. 18, pp. 1691-1706, 1989.
- Brusseau, M.L., A.L. Wood, and P.S.C. Rao, "Influence of Organic Cosolvents on the Sorption Kinetics of Hydrophobic Organic Chemicals," Environmental Science and Technology, Vol. 25, pp. 903-910, 1991b.
- Carroll, K.M., M. R. Harkness, A.A. Bracco, and R.R. Balcarcel, "Application of a Permanent/Polymer Diffusional Model to the Desorption of Polychlorinated Biphenyls from Hudson River Sediments," Environmental Science and Technology, Vol. 28, pp. 253-258, 1994.
- Chiou, C.T., L.J. Peters, and V.H. Freed, "A Physical Concept of Soil-Water Equilibria for Nonionic Organic Compounds," Science, Vol. 206, pp. 831-832, 1979.
- Chiou, C.T., P.E. Porter, and D.W. Schmedding, "Partition Equilibria of Nonionic Organic Compounds between Soil Organic Matter and Water," Environmental Science and Technology, Vol. 17, pp. 227-231, 1983.

- Chiou, Cary T., T.D. Shoup, and P.E. Porter, "Mechanistic Roles of Soil Humus and Minerals in the Sorption of Nonionic Organic Compounds from Aqueous and Organic Solutions," Organic Geochemistry, Vol. 8, pp. 9-14, 1985.
- Connaughton, D.F. J.R. Stedinger, L.W. Lion, and M.L. Shuler, "Description of Time-Varying Desorption Kinetics: Release of Naphthalene from Contaminated Soils," Environmental Science Technology, Vol. 27, pp. 2397-2403, 1993.
- Crank, J., The Mathematics of Diffusion, London: Oxford University Press, 1975.
- Crank, J. and C.S. Park, Eds. Diffusion in Polymers, New York: Academic Press, 1968.
- Crittenden, J.C., N.J. Hutzler, and D.G. Geyer, "Transport of Organic Compounds With Saturated Groundwater Flow: Model Development and Parameter Sensitivity," Water Resources Research, Vol. 23, pp. 271-284, 1986.
- deVenoge, T.P., Development of Synthetic Soils for Sorption Mass Transfer Model Validation, Thesis, Air Force Institute of Technology, Wright-Patterson Air Force Base OH, 1996.
- Farrell, J. and M. Reinhard, "Description of Halogenated Organics from Model Solids, Sediments, and Soil under Unsaturated Conditions. 2. Kinetics," Environmental Science Technology, Vol. 28, pp. 63-72, 1994.
- Garbarini, D.R., and L.W. Lion, "Influence of the Nature of Soil Organics on the Sorption of Toluene and Trichloroethylene," Environmental Science and Technology, Vol. 20, pp. 1263-1269, 1986.
- Gauthier, T.D., W.R. Seltz, and C.L. Grant, "Effect of Structural and Compositional Variations of Dissolved Humic Materials on Pyrene K_{oc} Values," Environmental Science and Technology, Vol. 21, pp. 243-248, 1987.
- Goltz, M.N., Three-Dimensional Analytical Modeling of Diffusion-limited Transport, PhD, Stanford University, San Jose CA, 1986.
- Gschwend, P.M., and S.-C. Wu, "On the Constancy of Sediment-water Partition Coefficients of Hydrophobic Organic Pollutants," Environmental Science and Technology, Vol. 19, No. 1, pp. 90-96, 1985.
- Hamaker, J.W. and J. M. Thompson, Adsorption in Organic Chemicals in the Soil Environment, Vol. 6, C.A. Goring and J.W. Hamaker, Eds. pp. 49-143, New York: Marcel Dekker, Inc., 1972.

- Heyse, E., Mass Transfer between Organic and Aqueous Phases: Investigations using a Continuously Stirred Flow Cell, PhD Dissertation, University of Florida, Gainesville FL, 1994.
- Karickhoff, S.W., "Semi-Empirical Estimation of Sorption of Hydrophobic Pollutants On Natural Sediments and Soils," Chemosphere, Vol. 10, No. 8, pp. 833-846, 1981.
- Karickhoff, S.W., D.S. Brown, and T.A. Scott, "Sorption of Hydrophobic Pollutants on Natural Sediments," Water Research, Vol. 13, pp. 241-248, 1979.
- Karickhoff, S.W., and K.R. Morris, "Sorption Dynamics of Hydrophobic Pollutants in Sediment Suspensions," Environmental Toxicology Chemistry, Vol. 4, pp. 469-479, 1985.
- Kookana, Rai S., R.D. Schuller and L.A.G. Aylmore, "Simulation of simazine transport through soil columns using time-dependent sorption data measured under flow conditions," Journal of Contaminant Hydrology, Vol. 14, pp. 93-115, 1993.
- Lee, L.S., P.S.C. Rao, M.L. Brusseau, and R.A. Ogwada, "Nonequilibrium Sorption of Organic Contaminants During Flow Through Columns of Aquifer Materials," Environmental Toxicology and Chemistry, Vol. 7, pp. 779-793, 1988.
- Lion, L.W., T.B. Stauffer, and W.G. MacIntyre, "Sorption of Hydrophobic Compounds on Aquifer Materials," Journal of Contaminant Hydrology, Vol. 5 pp. 215-234, 1990.
- Meeter, D.A. and P.J. Wolfe, Supplemental Program Series 50, University of Wisconsin Computer Center, Madison, WI, 1968.
- Miller, C.T., Modelling of Sorption and Desorption Phenomena for Hydrophobic Organic Contaminants in Saturated Soil Environments, PhD Dissertation, University of Michigan, Ann Arbor, MI, 1984.
- Miller, C.T., and W.J. Weber Jr., "Modeling Organic Contaminant Partitioning in Ground-Water Systems," Ground Water, Vol. 22, pp. 584-592, 1984.
- Miller, C.T., and W.J. Weber Jr., "Sorption of Hydrophobic Organic Pollutants in Saturated Soil Systems," Journal of Contaminant Hydrology, Vol. 1, pp. 243-261, 1986.

- Nkedi-Kizza, P., M.L. Brusseau, P.S.C. Rao, and A.G. Hornsby, "Nonequilibrium Sorption during Displacement of Hydrophobic Organic Chemicals and ^{45}Ca through Soil Columns with Aqueous and Mixed Solvents," Environmental Science and Technology, Vol. 23, pp. 814-820, 1989.
- Parker, J.C. and A.J. Valocchi, "Constraints on the Validity of Equilibrium and First-Order Kinetic Transport Models in Structured Soils," Water Resources Research, Vol. 22, pp. 399-407, 1986.
- Pignatello, J.J., "Slowly Reversible Sorption of Aliphatic Halocarbons in Soils I. Formation of Residual Fractions," Environmental Toxicology and Chemistry, Vol. 9, pp. 1107-1115, 1990.
- Ramaswami, A., S. Ghoshal and R. G. Luthy, "Mass Transfer and Biodegradation of PAH Compounds from Coal Tar," Water Science Technology, Vol. 30, pp. 61-70, 1994.
- Rao, P.S.C, R.E. Jessup, D.E. Rolston, J.M. Davidson, and D. P. Kilcrease, "Experimental and Mathematical Description of Nonadsorbed Solute Transfer by Diffusion in Spherical Aggregates," Soil Science Society of America Journal, Vol. 44, pp. 684-688, 1980a.
- Rao, P.S.C, R.E. Jessup, and T.M. Addiscott, "Experimental and Theoretical Aspects of Solute Diffusion in Spherical and Nonpherical Aggregates," Soil Science, Vol. 133, pp. 342-349, 1982.
- Rao, P.S.C, D.E. Rolston, R.E. Jessup, and J.M. Davidson, "Solute Transport in Aggregated Porous Media: Theoretical and Experimental Evaluation," Soil Science Society of America Journal, Vol. 44, pp. 1139-1146, 1980b.
- Rebhun, M., R. Kalabo, L. Grossman, J. Manka, and Ch. Rav-Acha, "Sorption of Organics on Clay and Synthetic Humic-Clay Complexes Simulating Aquifer Processes," Water Research, Vol. 26, pp. 79-84, 1992.
- Roberts, P.V., M.N. Goltz, and D.M. Mackay, "A Natural Gradient Experiment on Solute Transport in a Sand Aquifer: 3. Retardation Estimates and Mass Balances for Organic Solutes," Water Resources Research, Vol. 22, pp. 2047-2058, 1986.
- Rounds, S.A., B.A. Tiffany, and J.F. Pankow, "Description of Gas/Particle Sorption Kinetics with Intraparticle Diffusion Model: Desorption Experiments," Environmental Science and Technology, Vol. 27, pp. 366-377, 1993.

- Rutherford, D.W., C.T. Chiou, and D.E. Kile, "Influence of Soil Organic Matter Composition on the Partition of Organic Compounds," Environmental Science and Technology, Vol. 26, pp. 336-340, 1992.
- Schwarzenbach, R.P. and J. Westall, "Transport of Nonpolar Organic Compounds from Surface Water to Groundwater: Laboratory Sorption Studies," Environmental Science and Technology, Vol. 15, pp. 1360-1367, 1981.
- Schwarzenbach, R.P., P.M. Gschwend, and D.M. Imboden. Environmental Organic Chemistry. New York: John Wiley and Sons, Inc., 1993.
- Scow, K.M., and M. Alexander, "Effect of Diffusion on the Kinetics of Biodegradation: Experimental Results with Synthetic Aggregates," Soil Science Society of America Journal Vol. 56, pp. 128-134, 1992.
- Scow, K.M., and J. Hutson, "Effect of Diffusion and Sorption on the Kinetics of Biodegradation: Theoretical Considerations," Soil Science Society of America Journal Vol. 56, pp. 119-127, 1992.
- Steinberg, S.M., J.J. Pignatello, and B.L. Sawhney, "Persistence of 1,2-dibromomethane in Soils: Entrapment in Intraparticle Micropores," Environmental Science and Technology, Vol. 21, pp. 1201-1208, 1987.
- Szecsody, J. E., Sorption Kinetics of Hydrophobic Organic Compounds Onto Organic Modified Surfaces, PhD Dissertation, University of Arizona, Tucson, 1988.
- van Genuchten, M. Th., J.M. Davidson and P.J. Wierenga, "An Evaluation of Kinetic and Equilibrium Equations for the Prediction of Pesticide Movement through Porous Media," Soil Science Society of America Journal, Vol. 38, pp. 29-35, 1974.
- van Genuchten, M. Th. and R.J. Wagenet, "Two-Site/Two-Region Models for Pesticide Transport and Degradation: Theoretical Development and Analytical Solutions," Soil Science Society of America Journal, Vol. 53, pp. 1303-1310, 1989.
- van Genuchten, M. Th. and P.J. Wierenga, "Mass Transfer Studies in Sorbing Porous Media I. Analytical Solutions," Soil Science Society of America Journal, Vol. 40, pp. 473-480, 1976.
- Weber, W.J., P.M. McGinley, and L.E. Katz, "Sorption Phenomena in Subsurface Systems: Concepts, Models and Effects on Contaminant Fate and Transport," Water Resources, Vol. 25, pp. 499-528, 1991.

- Woodburn, K.B., L.S. Lee, P.S.C. Rao, and J.J. Delfino, "Comparison of Sorption Energetics for Hydrophobic Organic Chemicals by Synthetic and Natural Sorbents from Methanol/Water Solvent Mixtures," Environmental Science and Technology, Vol. 23, pp. 407-413, 1989.
- Wu, s. and P.M. Gschwend, "Sorptions Kinetics of Hydrophobic Organic Compounds to Natural Sediments and Soils," Environmental Science and Technology, Vol. 20, pp. 717-725, 1986.
- Xing, B., J.J. Pignatello, and B. Gigliotti, "Competitive Sorption between Atrazine and Other Organic Compounds in Soils and Model Sorbents," Environmental Science and Technology, Vol. 30, pp. 2432-2440, 1996.
- Young, D.F., and W.P. Ball, "Effects of Column Conditions on the First-Order Rate Modeling of Nonequilibrium Solute Breakthrough," Water Resources Research, Vol. 31, pp. 2181-2192, 1995.

Appendix A: Glossary

Roman

b = radius of sphere, L

C = concentration of individual components, $M L^{-3}$

C_{im} = concentration (path length δ and time t) in the immobile liquid phase, $M L^{-3}$

$\overline{C_{im}}$ = average concentration in the immobile liquid phase, $M L^{-3}$

C_t = concentration of solute in solution, $M L^{-3}$

$C_{l(i)}$ = initial liquid phase concentration, $M L^{-3}$

C_m = concentration in the mobile liquid phase, $M L^{-3}$

C_{om} = concentration of sorbate associated with the SOM, $M L^{-3}$

$C_{s(f)}$ = final liquid phase concentration, $M L^{-3}$

D = diffusion coefficient, $L^2 t^{-1}$

D_a = apparent diffusion coefficient, $L^2 t^{-1}$

D_m = mobile region dispersion coefficient, $L^2 t^{-1}$

D_o = free-liquid diffusion coefficient, $L^2 t^{-1}$

f = fraction of sorption sites that are in contact with the mobile water phase

f_{oc} = fraction of organic carbon

f_{om} = weight fraction of solid which is SOM

F = fraction of sorption sites

J = mass flux, $M L^{-2} t^{-1}$

k_2 = first-order mass transfer rate coefficient, $L t^{-1}$

K_{ad} = equilibrium adsorption coefficient, $L^3 M^{-1}$

K_d = linear sorption distribution coefficient, $L^3 M^{-1}$

K_{oc} = organic carbon distribution coefficient, $L^3 M^{-1}$

K_p = equilibrium partition coefficient, $L^3 M^{-1}$

K_{ow} = octanol-water partition coefficient, $L^3 M^{-1}$

$M_l =$ mass of the liquid, M

$M_s =$ mass of the solid, M

$r =$ radial coordinate of the spherical particle, L

$t =$ time, t

$R =$ retardation factor

$S =$ sorbed concentration, $M M^{-1}$

$v =$ average pore water velocity, $L t^{-1}$

$V_s =$ bulk volume of ceramic sphere

$V_l =$ volume of the liquid, L^3

$x =$ distance, L

Greek

$\alpha' =$ first-order mass transfer coefficient, $L t^{-1}$

$\delta =$ diffusion path length, L

$\delta_{max} =$ maximum diffusion path length, L

$\lambda =$ shape factor

$\rho_b =$ bulk soil density, $M L^{-3}$

$\rho_l =$ density of the liquid, $M L^{-3}$

$\theta_m =$ mobile phase porosity, $L^3 L^{-3}$

$\theta_{im} =$ immobile phase porosity, $L^3 L^{-3}$

$\tau =$ tortuosity

Appendix B: Experiment Data

Table 1. Nylon-66 Isotherm Experiment

Liquid Phase Concentration of Anthracene	Contents of each Vial ~ 0.07 g crushed Nylon 66			
0.81 mg/L	BN-2A	BN-2B	BN-5A	BN-5B
0.61 mg/L	BN-2A	BN-2B	BN-5A	BN-5B
0.41 mg/L	BN-2A	BN-2B	BN-5A	BN-5B
0.20 mg/L	BN-2A	BN-2B	BN-5A	BN-5B
0.0 mg/L	BN-2		BN-5	

Table 2. Nylon-66 Rate Experiment (BN1.5 -BN5)

Size of Nylon 66 Sphere (cm)	Quantity of Spheres per Vial	Initial Concentration of Liquid Phase (mg/L)	Quantity of Vials	Mass of Solid Phase (g)
0.238	71	0.81	3	0.572
0.318	30	0.81	3	0.578
0.476	9	0.81	3	0.560
0.635	4	0.81	3	0.612
0.794	2	0.81	3	0.596
mixed sizes	3 (0.238), 2 (0.318), 1 (0.476), 1 (0.635), 1 (0.794)	0.81	3	0.576
mixed blank	3 (0.238), 2 (0.318), 1 (0.476), 1 (0.635), 1 (0.794)	0.81	2	0.576

Table 3. Porous Ceramic Sphere Rate Experiment (SB and LB)

Size of Porous Ceramic Sphere (cm)	Quantity of Spheres per Vial	Initial Concentration of Liquid Phase (mg/L)	Quantity of Vials or Bottles	Volume of Liquid Phase (mL)
0.55	8	0.80	2	19.0
0.75	6	0.80	2	35.0

Table 4. Mixed Porous Ceramic and Paraffin Sphere Rate Experiment (PMB)

Size of Sphere (cm)	Quantity of Spheres per Vial	Initial Concentration of Liquid Phase (mg/L)	Quantity of Vials	Volume of Liquid Phase (mL)
0.55, 0.75, ceramic and 0.249 paraffin	6 (0.55), 3 (0.75), and 7 (0.249)	0.80	2	31.0

Appendix C: MSS Model Code

```
MSSFIT
C
C Program Testfit
C
C Adapted for CSTR experiencing:
C Multisite (series) sorption on soil (spherical distribution)
C Flow and inlet concentration perturbations
C Bicontinuum sorption on reactor walls
C
C NUMERICAL SOLUTION
C
C BY: E. Heyse
C University of Florida, 23 AUG 93
C
C
C dim scrat = 5*np + np*np + (2+np)*nob
C signs = 1 means parms cannot change sign
C P(IPOINT(I)) = VAL(I) == PNAME(I)
C
C IMPLICIT DOUBLE PRECISION (A-H,O-Z)
DOUBLE PRECISION FOC,XM,V,PC0,TBCC(30),XQ(30),XCIN(30)
DOUBLE PRECISION VR(30),VA(30),CA(30),FAST
DOUBLE PRECISION XMR,XKPR,XKR,XFR,X(100),XKP,DEFF,DPATH,XSS0,XSR0
DIMENSION IX(100),Y(100),P(7),DIFF(7),SIGNS(7),SCRAT(1999)
DIMENSION IFC(30)
CHARACTER*8 PNAME(7)
CHARACTER*15 INFIL,OUT1,OUT2
DIMENSION VAL(7),IPOINT(7),IVARY(7)
COMMON /BMOD/FOC,XM,V,PC0,NEFD,TBCC,XQ,XCIN,VR,VA,CA
COMMON /BMODA/XMR,XKPR,XKR,XFR,NFRAC,IFLAG
COMMON /VALUE/ VAL,IPOINT,IVARY,PNAME,NFIX
COMMON /BDAT/ IX,X
CHARACTER*80 TIT,LIN1,LIN2,LIN3,LIN4
NFIX=6
PNAME(1)=' Kd '
PNAME(2)=' Deff '
PNAME(3)=' dpath '
PNAME(4)=' Lambda '
PNAME(5)=' Ss0 '
PNAME(6)=' Fast '
WRITE(*,*) 'NAME OF INPUT FILE?'
READ(5,1111)INFIL
1111 FORMAT(A15)
WRITE(6,*)'NAME OF SHORT OUTPUT FILE?'
READ(5,1111)OUT1
```



```

WRITE(6,*)'NAME OF LONG OUTPUT FILE?'
READ(5,1111)OUT2
OPEN(UNIT=3,FILE=INFIL,STATUS='OLD')
OPEN(UNIT=10,FILE=OUT1,STATUS='NEW')
OPEN(UNIT=4,FILE=OUT2,STATUS='NEW')
READ(3,'(A)') TIT
C
C   Read parameters to be fitted
C
C   RKD = partition coefficient, KP,
C   DEFF = Coefficient of Diffusion, D_eff cm^2/sec
C   DPATH = Total diff. path length, d, cm
C   RLAM = shape factor Lambda
C   XSS0 = Initial dmls Concentration in slow soil sites, Sso, ug/g
C   FAST = Fraction of equilibrium sorption sites
C
READ(3,'(A)') LIN1
READ(3,*) RKD,DEFF,DPATH,RLAM,XSS0,FAST
C
C   Read Constants
C
C   FOC = Mass fraction organic carbon on soil, foc
C   XM = Mass of soil in reactor, g
C   V = Volume of solvent in reactor at time zero, mL
C   PC0 = initial concentration in liquid, mg/l
C   NEFD = Number of boundary condition changes
C   IFC = boundary condition number
C   TBCC = time for boundary condition to end
C   XQ = Flow rate, mL/min
C   XCIN = Dimensionless inlet concentration
C   XMR = Mass of reactor, g
C   XKPR = Linear partition coef. on reactor, mL/g
C   XKR = 1st order mass transfer rate onto reactor, min^-1
C   XFR = Fraction instantaneous sorbing reactor sites
C   VS(J) = volume of liquid in rx for BC period j, ml
C   VR(J) = volume of liquid removed at end of BC period J, ml.
C   VA(j) = volume of liquid added at end of BC period J, ml.
C   CA(J) = concentration in liquid added at end of BC period J,mg/l.
C   XIC = sorbed concentration in each slow compartment, ug/g
C   CL = current liquid concentration, mg/l
C
READ(3,'(A)') LIN2
READ(3,*) (IVARY(I),I=1,NFIX)
READ(3,'(A)') LIN3
READ(3,*) XM,V,PC0
C   READ(3,*) XMR,XKPR,XKR,XFR
READ(3,*) NEFD

```

```

      DO 6 I=1,NEFD
6 READ(3,*) IFC(I),TBCC(I),VR(I),VA(I),CA(I)
C   Read numerical parameter
C   IFLAG=0 for sorbed/liquid concentration
C   IFLAG=1 for liquid concentration
      READ(3,*)NFRAC,IFLAG
C
C   Read Data to be fitted
C
C   X = time, seconds
C   Y = observation at time X, see IFLAG.
C
      READ(3,'(A)') LIN4
      NOB=0
      DO 3 I=1,100
      READ(3,*,END=4) X(I),Y(I)
3   NOB=NOB+1
4   WRITE(4,1) TIT
1   FORMAT(' ',A)
      WRITE(4,1) LIN1
      WRITE(4,2) RKD,DEFF,DPATH,RLAM,XSS0,FAST
2   FORMAT(' ',7E12.6)
      WRITE(4,1) LIN2
      WRITE(4,5) (IVARY(I),I=1,NFIX)
5   FORMAT(' ',7I10)
      WRITE(4,1) LIN3
      WRITE(4,777) XM,V,PC0,NEFD
777 FORMAT(' ',3E12.6,/,I10)
      DO 778 I=1,NEFD
      WRITE(4,779) IFC(I),TBCC(I),VR(I),VA(I),CA(I)
778 CONTINUE
779 FORMAT(' ',I10,4E12.6)
      VAL(1)=RKD
      VAL(2)=DEFF
      VAL(3)=DPATH
      VAL(4)=RLAM
      VAL(5)=XSS0
      VAL(6)=FAST
      NP=0
      JFIX=NFIX
      DO 20 I=1,NFIX
      IF (IVARY(I).EQ.1) THEN
          NP=NP+1
          IPOINT(I)=NP
      ELSE
          IPOINT(I)=JFIX
          JFIX=JFIX-1

```

```

        ENDIF
20  CONTINUE
    DO 22 I=1,NFIX
        P(IPOINT(I))=VAL(I)
22  CONTINUE
    NPROB=1
    MIT=0
    EPS1=0.0
    EPS2=0.0
    FLAM=0.0
    IF(EPS1.LT.1.E-9) EPS1=0.0
    IF(EPS2.LT.1.E-9) EPS2=1.E-3
    IF(MIT.EQ.0) MIT=15
    IF(FLAM.LT.1.E-9) FLAM=0.01
    FNU=10.
    DO 9 I=1,6
        SIGNS(I)=1.0
9  DIFF(I)=0.01
    WRITE(4,7) NPROB
7  FORMAT(' PROBLEM NUMBER',I3,T26,'X',T38,'Y')
    WRITE(4,8) (X(I),Y(I),I=1,NOB)
8  FORMAT(' ',T19,2E12.5)
    WRITE(*,12) (PNAME(I),I=1,NFIX)
    WRITE(10,12) (PNAME(I),I=1,NFIX)
12  FORMAT(/T6,'SSQ',T11,7A12)
    WRITE(*,15) (P(IPOINT(I)),I=1,NFIX)
    WRITE(10,15) (P(IPOINT(I)),I=1,NFIX)
15  FORMAT(T11,7E12.5)
    CALL UWHAUS(NPROB,NOB,Y,NP,P,DIFF,SIGNS,EPS1,EPS2,MIT,FLAM,
    *FNU,SCRAT)
    WRITE(*,14) TIT
    WRITE(10,14) TIT
14  FORMAT(/' END: ',A)
999 STOP
    END

```

```

SUBROUTINE UWHAUS(NPROB,NOB,Y,NP,TH,DIFF,SIGNS,EPS1,EPS2,
1  MIT, FLAM, FNU, SCRAT)
DIMENSION SCRAT(1),Y(1),TH(1),DIFF(1),SIGNS(1)
IA=1
IB=IA+NP
IC=IB+NP
ID=IC+NP
IE=ID+NP
IF=IE+NP
IG=IF+NOB
IH=IG+NOB

```

```

II = IH + NP * NOB
IJ = IH
  CALL HAUS59(NPROB,NOB,Y,NP,TH,DIFF,SIGNS,EPS1,EPS2,MIT
1  ,FLAM,FNU,SCRAT(IA), SCRAT(IB), SCRAT(IC), SCRAT(ID),
2  SCRAT(IE), SCRAT(IF), SCRAT(IG), SCRAT(IH), SCRAT(II),
3  SCRAT(IJ) )
RETURN
END
SUBROUTINE HAUS59(NPRBO, NBO, Y,NQ,TH,DIFZ,SIGNS,EP1S,EP2S,
1MIT,FLAM,FNU, Q,P,E,PHI,TB,F,R,A,D,DELZ)
DIMENSION TH(1), DIFZ(1), SIGNS(1), Y(1), Q(1), P(1), E(1),
1 PHI(1), TB(1), F(1), R(1), A(1), D(1), DELZ(1)
CHARACTER*8 PNAME(7)
DIMENSION VAL(7),IPOINT(7),IVARY(7)
COMMON /VALUE/ VAL,IPOINT,IVARY,PNAME,NFIX
DATA MAXCNT/6/
ACOS(X) = ATAN(SQRT(1.0/X**2 - 1.0))
NP = NQ
NPROB = NPRBO
NOB = NBO
EPS1 = EP1S
EPS2 = EP2S
NPSQ = NP * NP
NSCRAC = 5*NP+NPSQ +2*NOB+NP*NOB
WRITE(4, 1000) NPROB, NOB, NP, NSCRAC
WRITE(4, 1001)
CALL GASS60(1, NP, TH, TEMP, TMEP)
WRITE(4, 1002)
CALL GASS60(1, NP, DIFZ, TEMP, TEMP)
IF(MIN0(NP-1,50-NP,NOB-NP,MIT-1,999-MIT))99,15,15
15 IF(FNU-1.0)99, 99, 16
16 CONTINUE
DO 19 I=1,NP
TEMP = ABS(DIFZ(I))
IF(AMIN1(1.0-TEMP, ABS(TH(I))))99, 99, 19
19 CONTINUE
GA = FLAM
NIT = 1
ASSIGN 131 TO LAOS
ASSIGN 225 TO IRAN
ASSIGN 265 TO JORDAN
IF(EPS1) 5, 10, 10
5 EPS1 = 0
10 IF(EPS2) 40, 40, 30
40 IF(EPS1) 60, 60, 50
60 ASSIGN 270 TO IRAN
GO TO 70

```

```

50 ASSIGN 265 TO IRAN
   GO TO 70
30 IF(EPS1) 80, 80, 70
   80 ASSIGN 270 TO JORDAN
   70 SSQ = 0
     DO 71 I=1,NFIX
       IF(IVARY(I).EQ.1) VAL(I)=TH(IPOINT(I))
71 CONTINUE
   CALL MODEL(NPROB, TH, F, NOB, NP)
   DO 90 I = 1, NOB
     R(I) = Y(I) - F(I)
90 SSQ=SSQ+R(I)*R(I)
   WRITE(4, 1003) SSQ
   WRITE(*,3003) SSQ,(TH(IPOINT(I)),I=1,NFIX)
   WRITE(10,3003) SSQ,(TH(IPOINT(I)),I=1,NFIX)
3003 FORMAT(' ',1PE9.2,0P7E12.5)
   WRITE(4, 1011)
   WRITE(4, 2006) (F(I),I=1,NOB)
C           BEGIN ITERATION
100 GA = GA / FNU
   INTCNT = 0
   WRITE(4, 1004) NIT
101 JS = 1 - NOB
   DO 130 J=1,NP
     TEMP = TH(J)
     P(J)=DIFZ(J)*TH(J)
     TH(J)= TH(J)+P(J)
     Q(J)=0
     JS = JS + NOB
   DO 102 I=1,NFIX
     IF(IVARY(I).EQ.1) VAL(I)=TH(IPOINT(I))
102 CONTINUE
   CALL MODEL(NPROB, TH, DELZ(JS), NOB, NP)
   IJ = JS-1
   DO 120 I = 1, NOB
     IJ = IJ + 1
     DELZ(IJ) = DELZ(IJ) - F(I)
120 Q(J) = Q(J) + DELZ(IJ) * R(I)
     Q(J)= Q(J)/P(J)
C           Q=XT*R (STEEPEST DESCENT)
130 TH(J) = TEMP
   GO TO LAOS,(131,414)
131 DO 150 I = 1, NP
     DO 151 J=1,I
       SUM = 0
       KJ = NOB*(J-1)
       KI = NOB*(I-1)

```

```

DO 160 K = 1, NOB
KI = KI + 1
KJ = KJ + 1
160 SUM = SUM + DELZ(KI) * DELZ(KJ)
TEMP = SUM / (P(I) * P(J))
JI = J + NP * (I - 1)
D(JI) = TEMP
IJ = I + NP * (J - 1)
151 D(IJ) = TEMP
150 E(I) = SQRT(D(JI))
666 CONTINUE
DO 153 I = 1, NP
IJ = I - NP
DO 153 J = 1, I
IJ = IJ + NP
A(IJ) = D(IJ) / (E(I) * E(J))
JI = J + NP * (I - 1)
153 A(JI) = A(IJ)
C                                A = SCALED MOMENT MATRIX
II = - NP
DO 155 I = 1, NP
P(I) = Q(I) / E(I)
PHI(I) = P(I)
II = NP + 1 + II
155 A(II) = A(II) + GA
I = 1
CALL MATIN(A, NP, P, I, DET)
C                                P/E = CORRECTION VECTOR
STEP = 1.0
SUM1 = 0.
SUM2 = 0.
SUM3 = 0.
DO 231 I = 1, NP
SUM1 = P(I) * PHI(I) + SUM1
SUM2 = P(I) * P(I) + SUM2
SUM3 = PHI(I) * PHI(I) + SUM3
231 PHI(I) = P(I)
TEMP = SUM1 / SQRT(SUM2 * SUM3)
TEMP = AMIN1(TEMP, 1.0)
TEMP = 57.295 * ACOS(TEMP)
WRITE(4, 1041) DET, TEMP
170 DO 220 I = 1, NP
P(I) = PHI(I) * STEP / E(I)
TB(I) = TH(I) + P(I)
220 CONTINUE
WRITE(4, 7000)
7000 FORMAT(' TEST POINT PARAMETER VALUES')

```

```

WRITE(4, 2006) (TB(I), I = 1, NP)
DO 221 I = 1, NP
IF(SIGNS(I)) 221, 221, 222
222 IF(SIGN(1.0,TH(I))*SIGN(1.0,TB(I))) 663, 221, 221
221 CONTINUE
SUMB=0
DO 223 I=1,NFIX
IF(IVARY(I).EQ.1) VAL(I)=TB(IPOINT(I))
223 CONTINUE
CALL MODEL(NPROB, TB, F, NOB, NP)
DO 230 I=1,NOB
R(I)=Y(I)-F(I)
230 SUMB=SUMB+R(I)*R(I)
WRITE(4, 1043) SUMB
WRITE(*,3002) SUMB,(VAL(I),I=1,NFIX)
WRITE(10,3002) SUMB,(VAL(I),I=1,NFIX)
3002 FORMAT(' ',1PE9.2,0P7E12.5)
WRITE(4, 1011)
WRITE(4, 2006) (F(I),I=1,NOB)
IF(SUMB - (1.0+EPS1)*SSQ) 662, 662, 663
663 IF( AMIN1(TEMP-30.0, GA)) 665, 665, 664
665 STEP=STEP/2.0
INTCNT = INTCNT + 1
IF(INTCNT-MAXCNT) 170,2700,2700
664 GA=GA*FNU
INTCNT = INTCNT + 1
IF(INTCNT-MAXCNT) 666,2700,2700
662 WRITE(4, 1007)
DO 669 I=1,NP
669 TH(I)=TB(I)
CALL GASS60(1, NP, TH, TEMP, TEMP)
WRITE(4, 1040) GA, SUMB
GO TO IRAN,(225,270,265)
225 DO 240 I = 1, NP
IF(ABS(P(I))/(1.E-20+ABS(TH(I)))-EPS2) 240, 240, 241
241 GO TO JORDAN,(265,270)
240 CONTINUE
WRITE(4, 1009) EPS2
GO TO 280
265 IF(ABS(SUMB - SSQ) - EPS1*SSQ) 266, 266, 270
266 WRITE(4, 1010) EPS1
GO TO 280
270 SSQ=SUMB
NIT=NIT+1
IF(NIT - MIT) 100, 100, 280
2700 WRITE(4, 2710)

```

```

2710 FORMAT(/115H **** THE SUM OF SQUARES CANNOT BE REDUCED TO THE
SUM
10F SQUARES AT THE END OF THE LAST ITERATION - ITERATING STOPS /)
C          END ITERATION
280 WRITE(4, 1011)
    WRITE(4, 2001) (F(I), I = 1, NOB)
    WRITE(4, 1012)
    WRITE(4, 2001) (R(I), I = 1, NOB)
    SSQ=SUMB
    IDF=NOB-NP
    WRITE(4, 1015)
    I=0
    CALL MATIN(D, NP, P, I, DET)
    DO 7692 I=1,NP
    II = I + NP*(I-1)
7692 E(I) = SQRT(D(II))
    DO 340 I=1,NP
    JI = I + NP*(I-1) - 1
    IJ = I + NP*(I-2)
    DO 340 J = I, NP
    JI = JI + 1
    A(JI) = D(JI) / (E(I)*E(J))
    IJ = IJ + NP
340  A(IJ) = A(JI)
    CALL GASS60(3, NP, TEMP, TEMP, A)
    WRITE(4, 1016)
    CALL GASS60(1, NP, E, TEMP, TEMP)
    IF(IDF) 341, 410, 341
341  SDEV = SSQ / IDF
    WRITE(4, 1014) SDEV, IDF
    SDEV = SQRT(SDEV)
    WRITE(4,3007) (PNAME(I),I=1,NFIX)
    WRITE(*,3007) (PNAME(I),I=1,NFIX)
    WRITE(10,3007) (PNAME(I),I=1,NFIX)
3007 FORMAT(/T6,'SSQ',T11,7A12)
    DO 3008 I=1,NFIX
    IF(IVARY(I).EQ.1) VAL(I)=TH(IPOINT(I))
3008 CONTINUE
    WRITE(*,3004) SSQ,(VAL(I),I=1,NFIX)
    WRITE(10,3004) SSQ,(VAL(I),I=1,NFIX)
    WRITE(4,3004) SSQ,(VAL(I),I=1,NFIX)
3004 FORMAT(1PE10.2,0P7E12.5)
    DO 3005 I=1,NP
3005 P(I)=E(I)*SDEV
    DO 3009 I=1,NFIX
    VAL(I)=0.0
    IF(IVARY(I).EQ.1) VAL(I)=P(IPOINT(I))

```



```

3009 CONTINUE
      WRITE(*,3006) (VAL(I),I=1,NFIX)
      WRITE(10,3006) (VAL(I),I=1,NFIX)
      WRITE(4,3006) (VAL(I),I=1,NFIX)
3006 FORMAT(' Std. Dev.',7E12.5)
      DO 391 I=1,NP
        P(I)=TH(I)+2.0*E(I)*SDEV
391  TB(I)=TH(I)-2.0*E(I)*SDEV
      WRITE(4, 1039)
      CALL GASS60(2, NP, TB, P, TEMP)
C returns with out confidence limits on function values
      RETURN
      ASSIGN 414 TO LAOS
      GO TO 101
414 DO 415 K = 1, NOB
      TEMP = 0
      DO 420 I=1,NP
      DO 420 J=1,NP
      ISUB = K+NOB*(I-1)
      DEBUG1 = DELZ(ISUB)
      ISUB = K+NOB*(J-1)
      DEBUG2 = DELZ(ISUB)
      IJ = I + NP*(J-1)
      DEBUG3 = D(IJ)/(DIFZ(I)*TH(I)*DIFZ(J)*TH(J))
420  TEMP = TEMP + DEBUG1 * DEBUG2 * DEBUG3
      TEMP = 2.0*SQRT(TEMP)*SDEV
      R(K)=F(K)+TEMP
415  F(K)=F(K)-TEMP
      WRITE(4, 1008)
      IE=0
      DO 425 I=1,NOB,10
      IE=IE+10
      IF(NOB-IE) 430,435,435
430  IE=NOB
435  WRITE(4, 2001) (R(J), J = I, IE)
425  WRITE(4, 2006) (F(J), J = I, IE)
410  WRITE(4, 1033) NPROB
      RETURN
99  WRITE(4, 1034)
      GO TO 410
10000FORMAT(38H NON-LINEAR ESTIMATION, PROBLEM NUMBER I3,// I5,
  1 14H OBSERVATIONS, I5, 11H PARAMETERS I14, 17H SCRATCH REQUIRED)
1001 FORMAT(/25H INITIAL PARAMETER VALUES )
1002 FORMAT(/54H PROPORTIONS USED IN CALCULATING DIFFERENCE
QUOTIENTS )
1003 FORMAT(/25H INITIAL SUM OF SQUARES = E12.4)
1004 FORMAT(////45X,13H ITERATION NO. I4)

```

```

1007 FORMAT(/32H PARAMETER VALUES VIA REGRESSION )
1008 FORMAT(/54H APPROXIMATE CONFIDENCE LIMITS FOR EACH FUNCTION
VAL
1UE )
10090FORMAT(/62H ITERATION STOPS - RELATIVE CHANGE IN EACH PARAMETER
LE
1SS THAN E12.4)
10100FORMAT(/62H ITERATION STOPS - RELATIVE CHANGE IN SUM OF SQUARES
LE
1SS THAN E12.4)
1011 FORMAT(22H0 FUNCTION VALUES )
1012 FORMAT(/10H RESIDUALS )
1014 FORMAT(/24H VARIANCE OF RESIDUALS = ,E12.4,1H,I4,
120H DEGREES OF FREEDOM )
1015 FORMAT(/19H CORRELATION MATRIX )
1016 FORMAT(/21H NORMALIZING ELEMENTS )
1033 FORMAT(/19H END OF PROBLEM NO. I3)
1034 FORMAT(/16H PARAMETER ERROR )
10390FORMAT(/71H INDIVIDUAL CONFIDENCE LIMITS FOR EACH PARAMETER (ON
LI
1NEAR HYPOTHESIS) )
10400FORMAT(/9H LAMBDA =E10.3,40X,33HSUM OF SQUARES AFTER REGRESSION
=
1E15.7)
1041 FORMAT(14H DETERMINANT = E12.4, 6X, 25H ANGLE IN SCALED COORD. =
1 F5.2, 8HDEGREES )
1043 FORMAT(28H TEST POINT SUM OF SQUARES = E12.4)
2001 FORMAT(/10E12.4)
2006 FORMAT(/10E12.4)
END
SUBROUTINE MATIN(A, NVAR, B, NB, DET)
DIMENSION A(NVAR, 1), B(NVAR, 1)
PIVOTM = A(1,1)
DET = 1.0
DO 550 ICOL = 1, NVAR
PIVOT = A(ICOL, ICOL)
PIVOTM = AMIN1(PIVOT, PIVOTM)
DET = PIVOT * DET
C DIVIDE PIVOT ROW BY PIVOT ELEMENT
A(ICOL, ICOL) = 1.0
PIVOT = AMAX1(PIVOT, 1.E-20)
PIVOT = A(ICOL, ICOL)/PIVOT
DO 350 L=1,NVAR
350 A(ICOL, L) = A(ICOL, L)*PIVOT
IF(NB .EQ. 0) GO TO 371
DO 370 L=1,NB
370 B(ICOL, L) = B(ICOL, L)*PIVOT

```

```

C  REDUCE NON-PIVOT ROWS
371 DO 550 L1=1,NVAR
    IF(L1 .EQ. ICOL) GO TO 550
    T = A(L1, ICOL)
    A(L1, ICOL) = 0.
    DO 450 L=1,NVAR
450  A(L1, L) = A(L1, L) - A(ICOL, L)*T
    IF(NB .EQ. 0) GO TO 550
    DO 500 L=1,NB
500  B(L1, L) = B(L1, L)-B(ICOL,L)*T
550  CONTINUE
    RETURN
    END
    SUBROUTINE GASS60(ITYPE, NQ, A, B, C)
    DIMENSION A(NQ),B(NQ),C(NQ,NQ)
    NP = NQ
    NR = NP/10
    LOW = 1
    LUP = 10
10  IF( NR )15,20,30
15  RETURN
20  LUP=NP
    IF(LOW .GT. LUP) RETURN
30  WRITE(4, 500) (J,J=LOW,LUP)
    GO TO (40,60,80),ITYPE
40  WRITE(4, 600) (A(J),J=LOW,LUP)
    GO TO 100
60  WRITE(4, 600) (B(J),J=LOW,LUP)
    GO TO 40
80  DO 90 I=LOW,LUP
90  WRITE(4, 720) I,(C(J,I),J=LOW,I)
    LOW2=LUP+1
    IF(LOW2 .GT. NP) GO TO 100
    DO 95 I=LOW2,NP
95  WRITE(4, 720) I,(C(J,I),J=LOW,LUP)
100  LOW = LOW + 10
    LUP = LUP + 10
    NR = NR - 1
    GO TO 10
500  FORMAT(/I8,9I12)
600  FORMAT(10E12.4)
720  FORMAT(1H0,I3,1X,F7.4,9F12.4)
1  CONTINUE
    RETURN
    END
C THE MODEL

```

```

FDSOLVE
SUBROUTINE FDSOLVE(TIME,CTIME,ITSTEPS,ANS,XIC,
.FN,DELTA,CL,STOLD,VS)
C
C  IMPLICIT NONE
DOUBLE PRECISION ANS(101),XIC(101),
.DELTA(101),FN(101),K(101),RES(101),A(101),B(101),TIME,CTIME
.,RESN,DEFF,RKD,CL,FAST,ANS2
INTEGER ITSTEPS,NFRAC
DOUBLE PRECISION TBCC(30),XQ(30),XCIN(30),FOC,XM,V,PC0
DOUBLE PRECISION X(100),XMR,XKPR,XKR,XFR,DPATH,XSS0,XSR0
DOUBLE PRECISION SNEW(101),SOLD(101),STOLD,ST,VR(30)
DOUBLE PRECISION DELTAT,VS,VA(30),CA(30)
DIMENSION IX(100),Y(100),P(7),DIFF(7),SIGNS(7),SCRAT(1999)
DIMENSION IFC(30)
CHARACTER*8 PNAME(7)
DIMENSION VAL(7),IPOINT(7),IVARY(7)
COMMON /BMOD/FOC,XM,V,PC0,NEFD,TBCC,XQ,XCIN,VR,VA,CA
COMMON /BMODA/XMR,XKPR,XKR,XFR,NFRAC,IFLAG
COMMON /VALUE/ VAL,IPOINT,IVARY,PNAME,NFIX
COMMON /BDAT/ IX,X
C
C  DELTAT=(CTIME-TIME)/ITSTEPS
C
C  This version of FDSOLVE solves the compartment
C  equations using backward Euler time differencing
C  to avoid stability problems. The first-order
C  accuracy should be OK since it matches the first-order
C  spatial accuracy
C
C  Note a Gauss-Seidel solver is used to solve the
C  tridiagonal matrix system that results from the
C  Backward Euler application
C
C  Set initial conditions from XIC input
C  Also use this for initial guess for Gauss-Seidel solver
C
RKD=VAL(1)
DEFF=VAL(2)
DPATH=VAL(3)
RLAM=VAL(4)
XSS0=VAL(5)
FAST=VAL(6)
DO 10 I=1,NFRAC
SOLD(I)=XIC(I)
SNEW(I)=XIC(I)
10 CONTINUE

```

```

C
  NCOUNT=1
C
C
C   Set up constant used to avoid extra calculations
C   see Dave's notes
  K(1)=2.0*DEFF*DELTAT/(DELTA(1)**2)
  DO 20 J=2,NFRAC
    K(J)=2.0*DEFF*DELTAT/((DELTA(J-1)+DELTA(J))*DELTA(J))
  20 CONTINUE
C
C   Set up matrix constants
  DO 30 J=1,NFRAC-1
C   Diagonal term
  A(J)=1.0+K(J)+FN(J+1)*K(J+1)/FN(J)
  30 CONTINUE
C
  A(NFRAC)=1.0+K(NFRAC)
  DO 40 J=2,NFRAC
C   Subdiagonal term
  B(J)=-K(J)*FN(J)/FN(J-1)
  40 CONTINUE
C   Note that the super diagonal term is just
C   equal to -k(j), j=1,nfrac-1
C

  DO WHILE (NCOUNT.LE.ITSTEPS)
C
C   Gauss-Seidel iteration
  IGITER=0
  RESN=1.0
  DO WHILE((RESN.GT.0.00001).AND.(IGITER.LT.50))
C
  SNEW(1)=(K(2)*SNEW(2)+SOLD(1)+K(1)*FN(1)
    *RKD*(1.D0-FAST)*CL)/A(1)
C
  DO 50 J=2,NFRAC-1
    SNEW(J)=(SOLD(J)+K(J+1)*SNEW(J+1)-B(J)*SNEW(J-1))/A(J)
C
  50 CONTINUE
  SNEW(NFRAC)=(SOLD(NFRAC)-B(NFRAC)*SNEW(NFRAC-1))/A(NFRAC)
C
C   compute residual
C
  RESN=0.0
  RES(1)=A(1)*SNEW(1)-K(2)*SNEW(2)-
    SOLD(1)-K(1)*FN(1)*RKD*CL*(1.D0-FAST)

```

```

C
RESN=RESN+(RES(1))**2
C
DO 60 J=2,NFRAC-1
C
RES(J)=A(J)*SNEW(J)-K(J+1)*SNEW(J+1)+
B(J)*SNEW(J-1)-SOLD(J)
RESN=RESN+(RES(J)**2)
60 CONTINUE
C
RES(NFRAC)=A(NFRAC)*SNEW(NFRAC)+
B(NFRAC)*SNEW(NFRAC-1)-SOLD(NFRAC)
RESN=RESN+(RES(NFRAC)**2)
RESN=SQRT(RESN)
IGITER=IGITER+1
C
C End Gauss-Seidel loop
C
END DO
C
C Add the sorbed concentrations to update cl
C
ST=SNEW(1)
DO 70 J=2,NFRAC
ST=ST+SNEW(J)
70 CONTINUE
C
C Update the aqueous concentration using the
C sorbed concentration solutions
C
CL=CL+(XM/(VS+RKD*FAST*XM))*(STOLD-ST)
ANS(NCOUNT)=CL
ANS2=(ST+FAST*RKD*CL)/CL
IF (IFLAG.EQ.0) ANS(NCOUNT)=ANS2
C
DO 80 I=1,NFRAC
SOLD(I)=SNEW(I)
XIC(I)=SNEW(I)
80 CONTINUE
C
STOLD=ST
NCOUNT=NCOUNT+1
END DO
RETURN
END

```

```

SUBROUTINE INTERP(XT,TIME,CTIME,ANS,ITSTEPS,FR)
  DOUBLE PRECISION ANS(101),TIME,CTIME,XT,DELTAT
  DOUBLE PRECISION TIMEC
  INTEGER ITSTEP
C
  DELTAT=(CTIME-TIME)/ITSTEPS
  NCOUNT=0
  TIMEC=TIME
  DO WHILE (XT.GT.TIMEC)
    TIMEC=TIMEC+DELTAT
    NCOUNT=NCOUNT+1
  END DO
C  FR=(ANS(NCOUNT)+ANS(NCOUNT-1))/2.DO
  FR=(ANS(NCOUNT)-ANS(NCOUNT-1))*(XT-TIMEC+DELTAT)
  /DELTAT+ANS(NCOUNT-1)
  IF (XT.EQ.TIME) FR=ANS(1)
  IF (XT.EQ.CTIME) FR=ANS(ITSTEPS)
  RETURN
  END

```

```

INTF
SUBROUTINE INTF(RLAM,DELTA,DMAX,NFRAC,FN)
  DOUBLE PRECISION DELTA(100),FN(100),RLAM,DMAX
  INTEGER NFRAC
C
  FAC=(RLAM+1)/(DMAX**(RLAM+1))
  I=1
  X=0.0
  DO WHILE (I.LT.NFRAC)
C   Apply Simpson's rule
C   FN(I)=DELTA(I)*FAC/6.0*((DMAX-X)**RLAM+
C   .4.0*(DMAX-(X+DELTA(I)/2))**RLAM+
C   .(DMAX-(X+DELTA(I)))**RLAM)
  FN(I)=(((DMAX-X)**(RLAM+1.D0))-(DMAX-(X+DELTA(I)))**
  .(RLAM+1.D0))/(DMAX**(RLAM+1.D0))
  X=X+DELTA(I)
  I=I+1
  END DO
C   FN(NFRAC)=FAC*DELTA(NFRAC)
  FN(NFRAC)=(DELTA(NFRAC)**(RLAM+1.D0))/(DMAX**(RLAM+1.D0))
  RETURN
  END

```



```

BATCHI
PROGRAM MODEL
CDLC  SUBROUTINE MODEL (NPROB,P,F,NOB,NP)
C  IMPLICIT NONE
    DOUBLE PRECISION XIC(101),DELTA(101),
    . FN(101),RKD,CL
    INTEGER FDOMAIN
C
C
    DOUBLE PRECISION TBCC(30),XQ(30),XCIN(30),FOC,XM,V,PC0
    DOUBLE PRECISION X(100),XMR,XKPR,XKR,XFR,DEFF,DPATH,XSS0,XSR0
    DOUBLE PRECISION STOLD,VR(30),VS,VA(30),CA(30),Y(100)
    DOUBLE PRECISION ANS(101),TIME,CTIME,RLAM,FAST
    DIMENSION F(100),IFC(30)
C
    CHARACTER*8 PNAME(7)
    DIMENSION VAL(7),IPOINT(7),IVARY(7)
    COMMON /BMOD/FOC,XM,V,PC0,NEFD,TBCC,XQ,XCIN,VR,VA,CA
    COMMON /BMODA/XMR,XKPR,XKR,XFR,NFRAC,IFLAG
    COMMON /VALUE/ VAL,IPOINT,IVARY,PNAME,NFIX
    COMMON /BDAT/ IX,X
    CHARACTER*15 INFIL,OUT1,OUT2
    CHARACTER*80 TIT,LIN1,LIN2,LIN3,LIN4
    NFIX=6
    PNAME(1)=' Kd '
    PNAME(2)=' Deff '
    PNAME(3)=' dpath '
    PNAME(4)=' Lambda '
    PNAME(5)=' Ss0 '
    PNAME(6)=' Fast '
    WRITE(*,*) 'NAME OF INPUT FILE?'
    READ(5,1111)INFIL
1111 FORMAT(A15)
    WRITE(6,*)'NAME OF SHORT OUTPUT FILE?'
    READ(5,1111)OUT1
    OPEN(UNIT=3,FILE=INFIL,STATUS='OLD')
    OPEN(UNIT=10,FILE=OUT1,STATUS='NEW')
    READ(3,'(A)') TIT
    WRITE(10,*)TIT
    WRITE(10,*)' TIME          PREDICTED CONC  OBSERVED CONC'
C
C  Read parameters to be fitted
C
C  RKD = partition coefficient, KP,
C  DEFF = Coefficient of Diffusion, D_eff cm^2/sec
C  DPATH = Total diff. path length, d, cm
C  RLAM = shape factor Lambda

```

```

C   XSS0 = Initial dmIs Concentration in slow soil sites, Sso, ug/g
C   FAST = Fraction of equilibrium sorption sites
C
C   READ(3,'(A)') LIN1
C   READ(3,*) RKD,DEFF,DPATH,RLAM,XSS0,FAST
C
C   Read Constants
C
C   FOC = Mass fraction organic carbon on soil, foc
C   XM = Mass of soil in reactor, g
C   V = Volume of solvent in reactor at time zero, mL
C   PC0 = initial concentration in liquid, mg/l
C   NEFD = Number of boundary condition changes
C   IFC = boundary condition number
C   TBCC = time for boundary condition to end
C   XQ = Flow rate, mL/min
C   XCIN = Dimensionless inlet concentration
C   XMR = Mass of reactor, g
C   XKPR = Linear partition coef. on reactor, mL/g
C   XKR = 1st order mass transfer rate onto reactor, min^-1
C   XFR = Fraction instantaneous sorbing reactor sites
C   VS(J) = volume of liquid in rx for BC period j, ml
C   VR(J) = volume of liquid removed at end of BC period J, ml.
C   VA(j) = volume of liquid added at end of BC period J, ml.
C   CA(J) = concentration in liquid added at end of BC period J,mg/l.
C   XIC = sorbed concentration in each slow compartment, ug/g
C   CL = current liquid concentration, mg/l
C
C   READ(3,'(A)') LIN2
C   READ(3,*) (IVARY(I),I=1,NFIX)
C   READ(3,'(A)') LIN3
C   READ(3,*) XM,V,PC0
C   READ(3,*) XMR,XKPR,XKR,XFR
C   READ(3,*) NEFD
C   DO 6 I=1,NEFD
C   6 READ(3,*) IFC(I),TBCC(I),VR(I),VA(I),CA(I)
C   Read numerical parameter
C   IFLAG=0 for sorbed/liquid concentration
C   IFLAG=1 for liquid concentration
C   READ(3,*)NFRAC,IFLAG
C   CONTINUE
C
C   Read Data to be fitted
C
C   X = time, seconds
C   Y = observation at time X, see IFLAG.
C

```

```

READ(3,'(A)') LIN4
NOB=0
DO 3 I=1,100
READ(3,*,END=4) X(I),Y(I)
3 NOB=NOB+1
4 CONTINUE

C
C SET VAL PARAMETERS TO PASS TO SUBS
VAL(1)=RKD
VAL(3)=DPATH
VAL(2)=DEFF
VAL(4)=RLAM
VAL(5)=XSS0
VAL(6)=FAST

C
CDLC
C Begin new program for batch solution
C
C
C
C  $CL=(PC0*V+XM*XSS0*FAST)/(V+RKD*XM*FAST)$ 
VS=V

C
C Input the domain partitioning. Delta(I) is the delta for
C each compartment.
C
DO 10 I=1,NFRAC
DELTA(I)=DPATH/NFRAC
10 CONTINUE

C
C Subroutine INTF generates the F(i)'s by integrating f(delta)
C with RLAM as the shape parameter
C
C
C Set the initial condition within the immobile zone
C
C
CALL INTF(RLAM,DELTA,DPATH,NFRAC,FN)

C
C STOLD is the sum of the S for the diffusion compartments
C
STOLD=0.0
DO 20 I=1,NFRAC
XIC(I)=XSS0*FN(I)*(1.D0-FAST)
STOLD=STOLD+XIC(I)
20 CONTINUE

```

```

C
C   Loop through each flow domain
C
  FDOMAIN=1
  TIME=0.0
  IF (IFLAG.EQ.1) THEN
    WRITE(10,777)TIME,PC0
  ELSE
    WRITE(10,777)TIME,XSS0/PC0
  END IF

  IT=1
C   Note the the final time is X(NOBS)
  DO WHILE (FDOMAIN.LE.(NEFD+1))
C
C   ITSTEPS is the number of time steps per flow domain
C
  ITSTEPS=100
C
C   CTIME is the cumulative solution time
  CTIME=TBCC(FDOMAIN)
  IF (FDOMAIN.EQ.(NEFD+1)) CTIME=X(NOBS)
C   Check for short flow domains, and adjust time steps
  IF ((CTIME-TIME).LT.10.0) ITSTEPS=20
c
C   FDSOLVE computes the soln from time to ctime for itsteps and
C   passes the soln back as array ANS(ITSTEPS)
c
  CALL FDSOLVE(TIME,CTIME,ITSTEPS,ANS,XIC,
  FN,DELTA,CL,STOLD,VS)
C
C   INTERP interpolates the soln from FDSOLVE onto the observation
C   times and stores the results in array F(nobs)
C
  DO WHILE ((X(IT).LE.CTIME).AND.(X(IT).GE.TIME))
C   CALL INTERP(X(IT),TIME,CTIME,ANS,ITSTEPS,F(IT))
C   IT=IT+1
C   END DO
C   Write prediction data to output file
  PTIME=TIME
  DELTAT=(CTIME-TIME)/ITSTEPS
  DO 77 II=10,ITSTEPS,10
    PTIME=PTIME+10.D0*DELTAT
    WRITE(10,777)PTIME,ANS(II)
777  FORMAT(1X,2(E16.5))
77   CONTINUE

```

```

C
  TIME=CTIME
C
C   Adjust aqueous volume and new aqueous conc.
C
C
C
  CL=(VS*CL+VA(FDOMAIN)*CA(FDOMAIN)-VR(FDOMAIN)*CL)/
    (VS-VR(FDOMAIN)+VA(FDOMAIN))
  VS=VS-VR(FDOMAIN)+VA(FDOMAIN)
  FDOMAIN=FDOMAIN+1

C
  END DO
C
C   Output the results
C
  I=1
  DO WHILE (I.LT.NOB)
    WRITE(10,778)X(I),Y(I)
778  FORMAT(1X,E16.5,16X,E16.5)
    I=I+1
  END DO
  STOP
C  RETURN
  END

```

```

BATCHMSP
CDLC  PROGRAM MODEL
      SUBROUTINE MODEL (NPROB,P,F,NOB,NP)
C    IMPLICIT NONE
      DOUBLE PRECISION XIC(101),DELTA(101),
      FN(101),RKD,CL
      INTEGER FDOMAIN
C
C    Note for linking: I'm adding vr(30),va(30), and ca(30)
C    to common block bmod make sure that this mode is also
C    made to the caling program
C
      DOUBLE PRECISION TBCC(30),XQ(30),XCIN(30),FOC,XM,V,PC0
      DOUBLE PRECISION X(100),XMR,XKPR,XKR,XFR,DEFF,DPATH,XSS0,XSR0
      DOUBLE PRECISION STOLD,VR(30),VS,VA(30),CA(30),RK2(101)
      DOUBLE PRECISION ANS(101),TIME,CTIME,RLAM,FAST
      DIMENSION IX(100)
CDLC
      DIMENSION F(1),P(1)
C
      CHARACTER*8 PNAME(7)
      DIMENSION VAL(7),IPOINT(7),IVARY(7)
      COMMON /BMOD/FOC,XM,V,PC0,NEFD,TBCC,XQ,XCIN,VR,VA,CA
      COMMON /BMODA/XMR,XKPR,XKR,XFR,NFRAC,IFLAG
      COMMON /VALUE/ VAL,IPOINT,IVARY,PNAME,NFIX
      COMMON /BDAT/ IX,X
C
C    READ DATA FROM PARAMETERS
      RKD=VAL(1)
      DPATH=VAL(3)
      DEFF=VAL(2)
      RLAM=VAL(4)
      XSS0=VAL(5)
      FAST=VAL(6)

CDLC  Fake input data to make this a standalone program
CDLC  PC0=0.0
CDLC  NOB=10
CDLC  DO 100 I=1,NOB
CDLC    X(NOB)=1.0*I
CDLC 100 CONTINUE
CDLC  TBCC(1)=3.0
CDLC  TBCC(2)=2.0
CDLC  TBCC(3)=4.0
CDLC  TBCC(4)=1.0
CDLC  XM=.2
CDLC  V=.3

```

```

CDLC   DEFF=1.0
CDLC   RKD=1.0
CDLC   X(1)=.2
CDLC   X(2)=1.2
CDLC   X(3)=2.7
CDLC   X(4)=3.2
CDLC   X(5)=4.8
CDLC   X(6)=5.1
CDLC   X(7)=8.2
CDLC   X(8)=8.9
CDLC   X(9)=9.4
CDLC   X(10)=10.0
CDLC   RLAM=2.0
CDLC
C   Begin new program for batch solution
C
C   NFRAC is the number of compartments
CDLC   NFRAC=100
C
C   ED: RKD IS THE KD AND CL IS THE AQUEOUS CONC
C   VR is the volume removed per sample, change
C   this later to an array
C   VS is the current aqueous volume, modified as
C   samples are taken
C   VA is the volume added, CA is the conc of added
C   liquid.
C
C
C
CL=(PC0*V+XM*XSS0*FAST)/(V+RKD*XM*FAST)
VS=V
C
C   Input the domain partitioning. Delta(I) is the delta for
C   each compartment.
C
C   F0 is the max f value on the f vs delta plot
F0=(RLAM+1)/DPATH
DO 10 I=1,NFRAC
   DELTA(I)=F0/NFRAC
10 CONTINUE
C
C   Subroutine INTF generates the F(i)'s by integrating delta(f)
C   with RLAM as the shape parameter
C
C
C   Set the initial condition within the immobile zone
C
C

```

```

CALL INTF(RLAM,DELTA,DPATH,NFRAC,FN)
C
C STOLD is the sum of the S for the diffusion compartments
C Rk2(j) is the first order proportion constant for compartment j
STOLD=0.0
DO 20 I=1,NFRAC
  XIC(I)=XSS0*FN(I)*(1.D0-FAST)
  RK2(I)=(DEFF*DELTA(I)**2.D0)/(0.5D0*FN(I)**2.D0)
  STOLD=STOLD+XIC(I)
20 CONTINUE
C
C Loop through each flow domain
C
FDOMAIN=1
TIME=0.0
IT=1
C Note the the final time is X(NOBS)
DO WHILE (FDOMAIN.LE.(NEFD+1))
C
C ITSTEPS is the number of time steps per flow domain
C
ITSTEPS=100
C
C
C CTIME is the cumulative solution time
CTIME=TBCC(FDOMAIN)
IF (FDOMAIN.EQ.(NEFD+1)) CTIME=X(NOBS)
C Check for short flow domains, and adjust time steps
IF ((CTIME-TIME).LT.10.0) ITSTEPS=20
c
C FDSOLVE computes the soln from time to ctime for itsteps and
C passes the soln back as array ANS(ITSTEPS)
c
CALL FDSOLVE(TIME,CTIME,ITSTEPS,ANS,XIC,
FN,DELTA,CL,STOLD,VS,RK2)
C
C INTERP interpolates the soln from FDSOLVE onto the observation
C times and stores the results in array F(nobs)
C
DO WHILE ((X(IT).LE.CTIME).AND.(X(IT).GE.TIME))
  CALL INTERP(X(IT),TIME,CTIME,ANS,ITSTEPS,F(IT))
  IT=IT+1
END DO
TIME=CTIME
C
C Adjust aqueous volume and new aqueous conc.
C

```



```

C
C
  CL=(VS*CL+VA(FDOMAIN)*CA(FDOMAIN)-VR(FDOMAIN)*CL)/
  (VS-VR(FDOMAIN)+VA(FDOMAIN))
  VS=VS-VR(FDOMAIN)+VA(FDOMAIN)
  FDOMAIN=FDOMAIN+1

C
  END DO

C
C   Output the results
C
CDLC  I=1
CDLC  DO WHILE (I.LT.NOB)
CDLC  WRITE(*,*)I,F(I)
CDLC  I=I+1
CDLC  END DO
CDLC  STOP
      RETURN
      END

```

Appendix D: MSS Model Input Data

TEST FOR MSSFIT: Small Beads Vial SB1: Kp from experiment

RKD	DEFF	DPATH	RLAM	XSS0	FAST
0.425	1.0E-8	0.55	2.0	0.0	0.0

1 MEANS FIT PARAMETER, 0 MEANS KEEP IT FIXED

0 1 0 0 0 0

CONSTANTS(Ms, Vli, Cli)

6.272 20.5 0.8910

9

1 900. 0.8491 0. 0.

2 2700. 0.959 0. 0.

3 5400. 0.878 0. 0.

4 9000. 0.8602 0. 0.

5 12600. 0.868 0. 0.

6 16200. 0.874 0. 0.

7 21600. 0.84 0. 0.

8 27000. 0.8591 0. 0.

9 32400. 0.851 0. 0.

100 0

TIME CONCENTRATION(Cs/Cw)

900. 0.0343

2700. 0.0443

5400. 0.0585

9000. 0.0789

12600. 0.0869

16200. 0.0999

21600. 0.1265

27000. 0.1390

32400. 0.1500

39600. 0.1644

TEST FOR MSSFIT: Small Beads Vial SB2: Kp from experiment

RKD DEFF DPATH RLAM XSS0 FAST
0.425 1.0E-8 0.55 2.0 0.0 0.0

1 MEANS FIT PARAMETER, 0 MEANS KEEP IT FIXED

0 1 0 0 0 0

CONSTANTS(Ms, Vli, Cli)

6.272 19.0 0.8910134

9

1 900. 0.8166 0. 0.

2 2700. 0.7362 0. 0.

3 5400. 0.779 0. 0.

4 9000. 0.7574 0. 0.

5 12600. 0.8365 0. 0.

6 16200. 0.8421 0. 0.

7 21600. 3.5689 0. 0.

8 27000. 0.8545 0. 0.

9 32400. 0.8474 0. 0.

100 0

TIME CONCENTRATION(Cs/Cw)

900. 0.06808

2700. 0.0784

5400. 0.0804

9000. 0.0962

12600. 0.1148

16200. 0.1276

21600. 0.1505

27000. 0.2344

32400. 0.1756

39600. 0.1946

TEST FOR MSSFIT: Small Beads Combined, Kp from experiment

RKD DEFF DPATH RLAM XSS0 FAST

0.425 1.0E-8 0.55 2.0 0.0 0.0

1 MEANS FIT PARAMETER, 0 MEANS KEEP IT FIXED

0 1 0 0 0 0

CONSTANTS(Ms, Vli, Cli)

2

6.272 20.5 0.8910 9.0

6.272 19.0 0.8910 10.0

1 900. 0.8491 0. 0.

2 2700. 0.959 0. 0.

3 5400. 0.878 0. 0.

4 9000. 0.8602 0. 0.

5 12600. 0.868 0. 0.

6 16200. 0.874 0. 0.

7 21600. 0.84 0. 0.

8 27000. 0.8591 0. 0.

9 32400. 0.851 0. 0.

10 39600. 0.8358 0. 0.

1 900. 0.8166 0. 0.

2 2700. 0.7362 0. 0.

3 5400. 0.779 0. 0.

4 9000. 0.7574 0. 0.

5 12600. 0.8365 0. 0.

6 16200. 0.8421 0. 0.

7 21600. 3.5689 0. 0.

8 27000. 0.8545 0. 0.

9 32400. 0.8474 0. 0.

100 0

TIME CONCENTRATION(Cs/Cw)

1 900. 0.0343

1 2700. 0.0443

1 5400. 0.0585

1 9000. 0.0789

1 12600. 0.0869

1 16200. 0.0999

1 21600. 0.1265

1 27000. 0.1390

1 32400. 0.1500

1 39600. 0.1644

1 90900. 0.1947

2 900. 0.06808

2 2700. 0.0784

2 5400. 0.0804

2 9000. 0.0962

2 12600. 0.1148

2 16200. 0.1276

2 21600. 0.1505
2 27000. 0.2344
2 32400. 0.1756
2 39600. 0.1946

TEST FOR MSSFIT: Large Beads Vial LB1: Kp from experiment

RKD DEFF DPATH RLAM XSS0 FAST

0.425 1.0E-8 0.75 2.0 0.0 0.0

1 MEANS FIT PARAMETER, 0 MEANS KEEP IT FIXED

0 1 0 0 0 0

CONSTANTS(Ms, Vli, Cli)

10.603 39.0 0.8027509

17

1 660. 0.8644 0. 0.

2 1320. 0.8644 0. 0.

3 1980. 0.8644 0. 0.

4 2700. 0.8644 0. 0.

5 3420. 0.8644 0. 0.

6 4140. 0.8644 0. 0.

7 7740. 0.8644 0. 0.

8 11340. 0.8644 0. 0.

9 14940. 0.8644 0. 0.

10 18540. 0.8644 0. 0.

11 22140. 0.8644 0. 0.

12 25740. 0.8644 0. 0.

13 29340. 0.8644 0. 0.

14 32940. 0.8644 0. 0.

15 61740. 0.8644 0. 0.

16 88080. 0.8644 0. 0.

17 220140. 0.8644 0. 0.

100 0

TIME CONCENTRATION(Cs/Cw)

660. 0.0596

1320. 0.0700

1980. 0.0722

2700. 0.1147

3420. 0.1080

4140. 0.1162

7740. 0.1523

11340. 0.1794

14940. 0.1820

18540. 0.1873

22140. 0.2132

25740. 0.2021

29340. 0.2305

32940. 0.2289

61740. 0.2869

88080. 0.3241

220140. 0.4234

988620. 0.4285

TEST FOR MSSFIT: Large Beads Vial LB2: Kp from experiment

RKD DEFF DPATH RLAM XSS0 FAST

0.425 10E-8 0.75 2.0 0.0 0.0

1 MEANS FIT PARAMETER, 0 MEANS KEEP IT FIXED

0 1 0 0 0 0

CONSTANTS(Ms, Vli, Cli)

10.603 39.0 0.8028

16

1 660. 0.8644 0. 0.

2 1320. 0.8644 0. 0.

3 1980. 0.8644 0. 0.

4 2640. 0.8644 0. 0.

5 4140. 0.8644 0. 0.

6 7740. 0.8644 0. 0.

7 11340. 0.8644 0. 0.

8 14940. 0.8644 0. 0.

9 18540. 0.8644 0. 0.

10 22140. 0.8644 0. 0.

11 25740. 0.8644 0. 0.

12 29340. 0.8644 0. 0.

13 32940. 0.8644 0. 0.

14 61740. 0.8644 0. 0.

15 88680. 0.8644 0. 0.

16 242880. 0.8644 0. 0.

100 0

TIME CONCENTRATION(Cs/Cw)

660. 0.0717

1320. 0.1012

1980. 0.1269

2700. 0.1492

4140. 0.1141

7740. 0.1540

11340. 0.1703

14940. 0.1761

18540. 0.1762

22140. 0.1959

25740. 0.2135

29340. 0.2161

32940. 0.2366

61740. 0.3004

88680. 0.3247

242880. 0.4126

991920. 0.4206

TEST FOR MSSFIT: Large Beads Combined

RKD DEFF DPATH RLAM XSS0 FAST
0.425 1.0E-8 0.75 2.0 0.0 0.0

1 MEANS FIT PARAMETER, 0 MEANS KEEP IT FIXED

0 1 0 0 0 0

CONSTANTS(Ms, Vli, Cli)

2

10.603 39.0 0.8028

17.0

10.603 39.0 0.8028 16.0

1 660. 0.8644 0. 0.

2 1320. 0.8644 0. 0.

3 1980. 0.8644 0. 0.

4 2700. 0.8644 0. 0.

5 3420. 0.8644 0. 0.

6 4140. 0.8644 0. 0.

7 7740. 0.8644 0. 0.

8 11340. 0.8644 0. 0.

9 14940. 0.8644 0. 0.

10 18540. 0.8644 0. 0.

11 22140. 0.8644 0. 0.

12 25740. 0.8644 0. 0.

13 29340. 0.8644 0. 0.

14 32940. 0.8644 0. 0.

15 61740. 0.8644 0. 0.

16 88080. 0.8644 0. 0.

17 220140. 0.8644 0. 0.

1 660. 0.8644 0. 0.

2 1320. 0.8644 0. 0.

3 1980. 0.8644 0. 0.

4 2640. 0.8644 0. 0.

5 4140. 0.8644 0. 0.

6 7740. 0.8644 0. 0.

7 11340. 0.8644 0. 0.

8 14940. 0.8644 0. 0.

9 18540. 0.8644 0. 0.

10 22140. 0.8644 0. 0.

11 25740. 0.8644 0. 0.

12 29340. 0.8644 0. 0.

13 32940. 0.8644 0. 0.

14 61740. 0.8644 0. 0.

15 88680. 0.8644 0. 0.

16 242880. 0.8644 0. 0.

100 0

TIME CONCENTRATION(Cs/Cw)

1 660. 0.0596

1 1320. 0.0700

1 1980. 0.0722
1 2700. 0.1147
1 3420. 0.1080
1 4140. 0.1162
1 7740. 0.1523
1 11340. 0.1794
1 14940. 0.1820
1 18540. 0.1873
1 22140. 0.2132
1 25740. 0.2021
1 29340. 0.2305
1 32940. 0.2289
1 61740. 0.2869
1 88080. 0.3241
1 220140. 0.4234
1 988620. 0.4285
2 660. 0.0717
2 1320. 0.1012
2 1980. 0.1269
2 2700. 0.1492
2 4140. 0.1141
2 7740. 0.1540
2 11340. 0.1703
2 14940. 0.1761
2 18540. 0.1762
2 22140. 0.1959
2 25740. 0.2135
2 29340. 0.2161
2 32940. 0.2366
2 61740. 0.3004
2 88680. 0.3247
2 242880. 0.4126
2 991920. 0.4206

TEST FOR MSSFIT: P Mixed Beads Vial PMB1: Kp from experiment

RKD DEFF DPATH RLAM XSS0 FAST

0.9158 1.0E-8 0.75 2.0 0.0 0.0

1 MEANS FIT PARAMETER, 0 MEANS KEEP IT FIXED

0 1 0 0 0 0

CONSTANTS(Ms, Vli, Cli)

13.381 39.0 0.8027509

18

1 720. 0.8870 0. 0.

2 1440. 0.8799 0. 0.

3 2100. 0.9395 0. 0.

4 2760. 0.8232 0. 0.

5 4260. 0.8242 0. 0.

6 7860. 0.8578 0. 0.

7 11460. 0.8314 0. 0.

8 15060. 0.7947 0. 0.

9 18660. 0.8429 0. 0.

10 22260. 0.8458 0. 0.

11 27660. 0.8307 0. 0.

12 33060. 1.0374 0. 0.

13 72960. 0.8308 0. 0.

14 111960. 0.8108 0. 0.

15 167520. 0.9417 0. 0.

16 530580. 0.8180 0. 0.

17 1394580. 0.8635 0. 0.

18 3295500. 0.8460 0. 0.

100 0

TIME CONCENTRATION(Cs/Cw)

720. 0.0236

1440. 0.0082

2100. 0.0134

2760. 0.024

4260. 0.0336

7860. 0.0257

11460. 0.0643

15060. 0.0783

18660. 0.0619

22260. 0.0697

27660. 0.0863

33060. 0.0952

72960. 0.166

111960. 0.2231

167520. 0.2758

530580. 0.4789

1394580. 0.7354

3295500. 0.9075

4151460. 0.9158

TEST FOR MSSFIT: P Mixed Beads Vial PMB2: Kp from experiment

RKD DEFF DPATH RLAM XSS0 FAST

0.8595 1.E-6 0.75 2.0 0.0 0.0

1 MEANS FIT PARAMETER, 0 MEANS KEEP IT FIXED

0 1 0 0 0 0

CONSTANTS(Ms,Vi,Cl)

13.381 31.0 0.8019

18

1 660. 0.7935 0. 0.

2 1320. 0.7945 0. 0.

3 1980. 0.8462 0. 0.

4 2640. 0.9261 0. 0.

5 3900. 0.7889 0. 0.

6 7500. 0.8163 0. 0.

7 11100. 0.8398 0. 0.

8 14700. 0.8121 0. 0.

9 18300. 0.8150 0. 0.

10 21900. 0.8221 0. 0.

11 27660. 1.1298 0. 0.

12 33060. 1.0613 0. 0.

13 69000. 0.8380 0. 0.

14 108660. 0.8415 0. 0.

15 151860. 0.8327 0. 0.

16 514920. 0.8637 0. 0.

17 1378920. 0.8561 0. 0.

18 3279840. 0.9363 0. 0.

100 0

TIME CONCENTRATION(Cs/Cw)

660. 0.0166

1320. 0.0184

1980. 0.0254

2640. 0.0251

3900. 0.0333

7500. 0.0895

11100. 0.0554

14700. 0.1077

18300. 0.0794

21900. 0.0935

27660. 0.1419

33060. 0.1167

69000. 0.1766

108660. 0.2594

151860. 0.3428

514920. 0.5371

1378920. 0.7964

3279840. 0.8671

4146780. 0.8595

TEST FOR MSSFIT: P Mixed Beads Vial Combined

RKD DEFF DPATH RLAM XSS0 FAST
0.88765 1.0E-8 0.75 2.0 0.0 0.0

1 MEANS FIT PARAMETER, 0 MEANS KEEP IT FIXED

0 1 0 0 0 0

CONSTANTS(Ms, Vli, Cli)

2

13.381 39.0 0.8027509 18.0

13.381 31.0 0.8019 18.0

1 720. 0.8870 0. 0.

2 1440. 0.8799 0. 0.

3 2100. 0.9395 0. 0.

4 2760. 0.8232 0. 0.

5 4260. 0.8242 0. 0.

6 7860. 0.8578 0. 0.

7 11460. 0.8314 0. 0.

8 15060. 0.7947 0. 0.

9 18660. 0.8429 0. 0.

10 22260. 0.8458 0. 0.

11 27660. 0.8307 0. 0.

12 33060. 1.0374 0. 0.

13 72960. 0.8308 0. 0.

14 111960. 0.8108 0. 0.

15 167520. 0.9417 0. 0.

16 530580. 0.8180 0. 0.

17 1394580. 0.8635 0. 0.

18 3295500. 0.8460 0. 0.

1 660. 0.7935 0. 0.

2 1320. 0.7945 0. 0.

3 1980. 0.8462 0. 0.

4 2640. 0.9261 0. 0.

5 3900. 0.7889 0. 0.

6 7500. 0.8163 0. 0.

7 11100. 0.8398 0. 0.

8 14700. 0.8121 0. 0.

9 18300. 0.8150 0. 0.

10 21900. 0.8221 0. 0.

11 27660. 1.1298 0. 0.

12 33060. 1.0613 0. 0.

13 69000. 0.8380 0. 0.

14 108660. 0.8415 0. 0.

15 151860. 0.8327 0. 0.

16 514920. 0.8637 0. 0.

17 1378920. 0.8561 0. 0.

18 3279840. 0.9363 0. 0.

100 0

TIME CONCENTRATION(Cs/Cw)

1 720. 0.0236
1 1440. 0.0082
1 2100. 0.0134
1 2760. 0.024
1 4260. 0.0336
1 7860. 0.0257
1 11460. 0.0643
1 15060. 0.0783
1 18660. 0.0619
1 22260. 0.0697
1 27660. 0.0863
1 33060. 0.0952
1 72960. 0.166
1 111960. 0.2231
1 167520. 0.2758
1 530580. 0.4789
1 1394580. 0.7354
1 3295500. 0.9075
1 4151460. 0.9158
2 660. 0.0166
2 1320. 0.0184
2 1980. 0.0254
2 2640. 0.0251
2 3900. 0.0333
2 7500. 0.0895
2 11100. 0.0554
2 14700. 0.1077
2 18300. 0.0794
2 21900. 0.0935
2 27660. 0.1419
2 33060. 0.1167
2 69000. 0.1766
2 108660. 0.2594
2 151860. 0.3428
2 514920. 0.5371
2 1378920. 0.7964
2 3279840. 0.8671
2 4146780. 0.8595

TEST FOR MSSFIT: Small Beads Vial SB1: Kp from experiment

RKD	DEFF	DPATH	RLAM	XSS0	FAST
0.425	0.12132E-6	0.55	2.0	0.0	0.0

1 MEANS FIT PARAMETER, 0 MEANS KEEP IT FIXED

0 0 1 1 0 0

CONSTANTS(Ms, Vli, Cli)

6.272 20.5 0.8910

10

1 900. 0.8491 0. 0.

2 2700. 0.959 0. 0.

3 5400. 0.878 0. 0.

4 9000. 0.8602 0. 0.

5 12600. 0.868 0. 0.

6 16200. 0.874 0. 0.

7 21600. 0.84 0. 0.

8 27000. 0.8591 0. 0.

9 32400. 0.851 0. 0.

10 39600. 0.8358 0. 0.

100 0

TIME CONCENTRATION(Cs/Cw)

900. 0.0343

2700. 0.0443

5400. 0.0585

9000. 0.0789

12600. 0.0869

16200. 0.0999

21600. 0.1265

27000. 0.1390

32400. 0.1500

39600. 0.1644

90900. 0.1947

TEST FOR MSSFIT: Small Beads Vial SB2: Kp from experiment

RKD DEFF DPATH RLAM XSS0 FAST

0.425 0.22469E-06 0.55 2.0 0.0 0.0

1 MEANS FIT PARAMETER, 0 MEANS KEEP IT FIXED

0 0 1 1 0 0

CONSTANTS(Ms, Vli, Cli)

6.272 19.0 0.8910134

10

1 900. 0.8166 0. 0.

2 2700. 0.7362 0. 0.

3 5400. 0.779 0. 0.

4 9000. 0.7574 0. 0.

5 12600. 0.8365 0. 0.

6 16200. 0.8421 0. 0.

7 21600. 3.5689 0. 0.

8 27000. 0.8545 0. 0.

9 32400. 0.8474 0. 0.

10 39600. 0.8471 0. 0.

100 0

TIME CONCENTRATION(Cs/Cw)

900. 0.06808

2700. 0.0784

5400. 0.0804

9000. 0.0962

12600. 0.1148

16200. 0.1276

21600. 0.1505

27000. 0.2344

32400. 0.1756

39600. 0.1946

90900. 0.2160

TEST FOR MSSFIT: Small Beads Combined

RKD DEFF DPATH RLAM XSS0 FAST
0.425 0.16507E-6 0.55 2.0 0.0 0.0

1 MEANS FIT PARAMETER, 0 MEANS KEEP IT FIXED

0 0 1 1 0 0

CONSTANTS(Ms, Vli, Cli)

2

6.272 20.5 0.8910 10.0

6.272 19.0 0.8910 10.0

1 900. 0.8491 0. 0.

2 2700. 0.959 0. 0.

3 5400. 0.878 0. 0.

4 9000. 0.8602 0. 0.

5 12600. 0.868 0. 0.

6 16200. 0.874 0. 0.

7 21600. 0.84 0. 0.

8 27000. 0.8591 0. 0.

9 32400. 0.851 0. 0.

10 39600. 0.8358 0. 0.

1 900. 0.8166 0. 0.

2 2700. 0.7362 0. 0.

3 5400. 0.779 0. 0.

4 9000. 0.7574 0. 0.

5 12600. 0.8365 0. 0.

6 16200. 0.8421 0. 0.

7 21600. 3.5689 0. 0.

8 27000. 0.8545 0. 0.

9 32400. 0.8474 0. 0.

10 39600. 0.8471 0. 0.

100 0

TIME CONCENTRATION(Cs/Cw)

1 900. 0.0343

1 2700. 0.0443

1 5400. 0.0585

1 9000. 0.0789

1 12600. 0.0869

1 16200. 0.0999

1 21600. 0.1265

1 27000. 0.1390

1 32400. 0.1500

1 39600. 0.1644

1 90900. 0.1947

2 900. 0.06808

2 2700. 0.0784

2 5400. 0.0804

2 9000. 0.0962

2 12600. 0.1148

2 16200. 0.1276
2 21600. 0.1505
2 27000. 0.2344
2 32400. 0.1756
2 39600. 0.1946
2 90900. 0.2160

TEST FOR MSSFIT: Large Beads Vial LB1: Kp from experiment

RKD DEFF DPATH RLAM XSS0 FAST

0.425 0.89949E-6 0.75 2.0 0.0 0.0

1 MEANS FIT PARAMETER, 0 MEANS KEEP IT FIXED

0 0 1 1 0 0

CONSTANTS(Ms, Vli, Cli)

10.603 39.0 0.8027509

17

1 660. 0.8644 0. 0.

2 1320. 0.8644 0. 0.

3 1980. 0.8644 0. 0.

4 2700. 0.8644 0. 0.

5 3420. 0.8644 0. 0.

6 4140. 0.8644 0. 0.

7 7740. 0.8644 0. 0.

8 11340. 0.8644 0. 0.

9 14940. 0.8644 0. 0.

10 18540. 0.8644 0. 0.

11 22140. 0.8644 0. 0.

12 25740. 0.8644 0. 0.

13 29340. 0.8644 0. 0.

14 32940. 0.8644 0. 0.

15 61740. 0.8644 0. 0.

16 88080. 0.8644 0. 0.

17 220140. 0.8644 0. 0.

100 0

TIME CONCENTRATION(Cs/Cw)

660. 0.0596

1320. 0.0700

1980. 0.0722

2700. 0.1147

3420. 0.1080

4140. 0.1162

7740. 0.1523

11340. 0.1794

14940. 0.1820

18540. 0.1873

22140. 0.2132

25740. 0.2021

29340. 0.2305

32940. 0.2289

61740. 0.2869

88080. 0.3241

220140. 0.4234

988620. 0.4285

TEST FOR MSSFIT: Large Beads Vial LB2: Kp from experiment

RKD DEFF DPATH RLAM XSS0 FAST

0.425 0.92897E-6 0.75 2.0 0.0 0.0

1 MEANS FIT PARAMETER, 0 MEANS KEEP IT FIXED

0 0 1 1 0 0

CONSTANTS(Ms, Vli, Cli)

10.603 39.0 0.8028

16

1 660. 0.8644 0. 0.

2 1320. 0.8644 0. 0.

3 1980. 0.8644 0. 0.

4 2640. 0.8644 0. 0.

5 4140. 0.8644 0. 0.

6 7740. 0.8644 0. 0.

7 11340. 0.8644 0. 0.

8 14940. 0.8644 0. 0.

9 18540. 0.8644 0. 0.

10 22140. 0.8644 0. 0.

11 25740. 0.8644 0. 0.

12 29340. 0.8644 0. 0.

13 32940. 0.8644 0. 0.

14 61740. 0.8644 0. 0.

15 88680. 0.8644 0. 0.

16 242880. 0.8644 0. 0.

100 0

TIME CONCENTRATION(Cs/Cw)

660. 0.0717

1320. 0.1012

1980. 0.1269

2700. 0.1492

4140. 0.1141

7740. 0.1540

11340. 0.1703

14940. 0.1761

18540. 0.1762

22140. 0.1959

25740. 0.2135

29340. 0.2161

32940. 0.2366

61740. 0.3004

88680. 0.3247

242880. 0.4126

991920. 0.4206

TEST FOR MSSFIT: Large Beads Combined

RKD	DEFF	DPATH	RLAM	XSS0	FAST
0.425	0.91935E-6	0.75	2.0	0.0	0.0

1 MEANS FIT PARAMETER, 0 MEANS KEEP IT FIXED

0 0 1 1 0 0

CONSTANTS(Ms, Vli, Cli)

2 10.603 39.0 0.8028
17.0 10.603 39.0 0.8028 16.0

1 660. 0.8644 0. 0.
2 1320. 0.8644 0. 0.
3 1980. 0.8644 0. 0.
4 2700. 0.8644 0. 0.
5 3420. 0.8644 0. 0.
6 4140. 0.8644 0. 0.
7 7740. 0.8644 0. 0.
8 11340. 0.8644 0. 0.
9 14940. 0.8644 0. 0.
10 18540. 0.8644 0. 0.
11 22140. 0.8644 0. 0.
12 25740. 0.8644 0. 0.
13 29340. 0.8644 0. 0.
14 32940. 0.8644 0. 0.
15 61740. 0.8644 0. 0.
16 88080. 0.8644 0. 0.
17 220140. 0.8644 0. 0.
1 660. 0.8644 0. 0.
2 1320. 0.8644 0. 0.
3 1980. 0.8644 0. 0.
4 2640. 0.8644 0. 0.
5 4140. 0.8644 0. 0.
6 7740. 0.8644 0. 0.
7 11340. 0.8644 0. 0.
8 14940. 0.8644 0. 0.
9 18540. 0.8644 0. 0.
10 22140. 0.8644 0. 0.
11 25740. 0.8644 0. 0.
12 29340. 0.8644 0. 0.
13 32940. 0.8644 0. 0.
14 61740. 0.8644 0. 0.
15 88680. 0.8644 0. 0.
16 242880. 0.8644 0. 0.

100 0

TIME CONCENTRATION(Cs/Cw)

1 660. 0.0596
1 1320. 0.0700
1 1980. 0.0722
1 2700. 0.1147

1 3420. 0.1080
1 4140. 0.1162
1 7740. 0.1523
1 11340. 0.1794
1 14940. 0.1820
1 18540. 0.1873
1 22140. 0.2132
1 25740. 0.2021
1 29340. 0.2305
1 32940. 0.2289
1 61740. 0.2869
1 88080. 0.3241
1 220140. 0.4234
1 988620. 0.4285
2 660. 0.0717
2 1320. 0.1012
2 1980. 0.1269
2 2700. 0.1492
2 4140. 0.1141
2 7740. 0.1540
2 11340. 0.1703
2 14940. 0.1761
2 18540. 0.1762
2 22140. 0.1959
2 25740. 0.2135
2 29340. 0.2161
2 32940. 0.2366
2 61740. 0.3004
2 88680. 0.3247
2 242880. 0.4126
2 991920. 0.4206

TEST FOR MSSFIT: P Mixed Beads Vial PMB1: Kp from experiment

RKD DEFF DPATH RLAM XSS0 FAST

0.888 1.16E-7 5.5 3.5 0.0 0.0

1 MEANS FIT PARAMETER, 0 MEANS KEEP IT FIXED

0 0 1 1 0 0

CONSTANTS(Ms, Vli, Cli)

13.381 39.0 0.8027509

18

1 720. 0.8870 0. 0.

2 1440. 0.8799 0. 0.

3 2100. 0.9395 0. 0.

4 2760. 0.8232 0. 0.

5 4260. 0.8242 0. 0.

6 7860. 0.8578 0. 0.

7 11460. 0.8314 0. 0.

8 15060. 0.7947 0. 0.

9 18660. 0.8429 0. 0.

10 22260. 0.8458 0. 0.

11 27660. 0.8307 0. 0.

12 33060. 1.0374 0. 0.

13 72960. 0.8308 0. 0.

14 111960. 0.8108 0. 0.

15 167520. 0.9417 0. 0.

16 530580. 0.8180 0. 0.

17 1394580. 0.8635 0. 0.

18 3295500. 0.8460 0. 0.

100 0

TIME CONCENTRATION(Cs/Cw)

720. 0.0236

1440. 0.0082

2100. 0.0134

2760. 0.024

4260. 0.0336

7860. 0.0257

11460. 0.0643

15060. 0.0783

18660. 0.0619

22260. 0.0697

27660. 0.0863

33060. 0.0952

72960. 0.166

111960. 0.2231

167520. 0.2758

530580. 0.4789

1394580. 0.7354

3295500. 0.9075

4151460. 0.9158

TEST FOR MSSFIT: P Mixed Beads Vial PMB2: Kp from experiment

RKD DEFF DPATH RLAM XSS0 FAST

0.888 1.16E-7 5.0 3.5 0.0 0.0

1 MEANS FIT PARAMETER, 0 MEANS KEEP IT FIXED

0 0 1 1 0 0

CONSTANTS(Ms, Vli, Cli)

13.381 31.0 0.8019

18

1 660. 0.7935 0. 0.

2 1320. 0.7945 0. 0.

3 1980. 0.8462 0. 0.

4 2640. 0.9261 0. 0.

5 3900. 0.7889 0. 0.

6 7500. 0.8163 0. 0.

7 11100. 0.8398 0. 0.

8 14700. 0.8121 0. 0.

9 18300. 0.8150 0. 0.

10 21900. 0.8221 0. 0.

11 27660. 1.1298 0. 0.

12 33060. 1.0613 0. 0.

13 69000. 0.8380 0. 0.

14 108660. 0.8415 0. 0.

15 151860. 0.8327 0. 0.

16 514920. 0.8637 0. 0.

17 1378920. 0.8561 0. 0.

18 3279840. 0.9363 0. 0.

100 0

TIME CONCENTRATION(Cs/Cw)

660. 0.0166

1320. 0.0184

1980. 0.0254

2640. 0.0251

3900. 0.0333

7500. 0.0895

11100. 0.0554

14700. 0.1077

18300. 0.0794

21900. 0.0935

27660. 0.1419

33060. 0.1167

69000. 0.1766

108660. 0.2594

151860. 0.3428

514920. 0.5371

1378920. 0.7964

3279840. 0.8671

4146780. 0.8595

TEST FOR MSSFIT: P Mixed Beads Vial Combined

RKD DEFF DPATH RLAM XSS0 FAST
0.888 1.16E-7 5.0 3.5 0.0 0.0

1 MEANS FIT PARAMETER, 0 MEANS KEEP IT FIXED

0 0 1 1 0 0

CONSTANTS(Ms, Vli, Cli)

2

13.381 39.0 0.8027509 18.0

13.381 31.0 0.8019 18.0

1 720. 0.8870 0. 0.

2 1440. 0.8799 0. 0.

3 2100. 0.9395 0. 0.

4 2760. 0.8232 0. 0.

5 4260. 0.8242 0. 0.

6 7860. 0.8578 0. 0.

7 11460. 0.8314 0. 0.

8 15060. 0.7947 0. 0.

9 18660. 0.8429 0. 0.

10 22260. 0.8458 0. 0.

11 27660. 0.8307 0. 0.

12 33060. 1.0374 0. 0.

13 72960. 0.8308 0. 0.

14 111960. 0.8108 0. 0.

15 167520. 0.9417 0. 0.

16 530580. 0.8180 0. 0.

17 1394580. 0.8635 0. 0.

18 3295500. 0.8460 0. 0.

1 660. 0.7935 0. 0.

2 1320. 0.7945 0. 0.

3 1980. 0.8462 0. 0.

4 2640. 0.9261 0. 0.

5 3900. 0.7889 0. 0.

6 7500. 0.8163 0. 0.

7 11100. 0.8398 0. 0.

8 14700. 0.8121 0. 0.

9 18300. 0.8150 0. 0.

10 21900. 0.8221 0. 0.

11 27660. 1.1298 0. 0.

12 33060. 1.0613 0. 0.

13 69000. 0.8380 0. 0.

14 108660. 0.8415 0. 0.

15 151860. 0.8327 0. 0.

16 514920. 0.8637 0. 0.

17 1378920. 0.8561 0. 0.

18 3279840. 0.9363 0. 0.

100 0

TIME CONCENTRATION(Cs/Cw)

1 720. 0.0236
1 1440. 0.0082
1 2100. 0.0134
1 2760. 0.024
1 4260. 0.0336
1 7860. 0.0257
1 11460. 0.0643
1 15060. 0.0783
1 18660. 0.0619
1 22260. 0.0697
1 27660. 0.0863
1 33060. 0.0952
1 72960. 0.166
1 111960. 0.2231
1 167520. 0.2758
1 530580. 0.4789
1 1394580. 0.7354
1 3295500. 0.9075
1 4151460. 0.9158
2 660. 0.0166
2 1320. 0.0184
2 1980. 0.0254
2 2640. 0.0251
2 3900. 0.0333
2 7500. 0.0895
2 11100. 0.0554
2 14700. 0.1077
2 18300. 0.0794
2 21900. 0.0935
2 27660. 0.1419
2 33060. 0.1167
2 69000. 0.1766
2 108660. 0.2594
2 151860. 0.3428
2 514920. 0.5371
2 1378920. 0.7964
2 3279840. 0.8671
2 4146780. 0.8595

Vita

Karla K. Mika [REDACTED] She graduated from Granite Hills High School in San Diego County, California in 1980 and entered the Air Force under the delayed enlisted program that same year. In April of 1981 she entered Basic Military Training where she was an Honor graduate in June 1980. She attended Technical Training at Sheppard AFB, Texas, and was awarded distinguished graduate.

Karla's first duty station was Ellsworth AFB, South Dakota where she worked in the Engineering and Environmental Planning Branch. Her second assignment was to the Air Force Engineering Liaison Office on Wheeler AFB, Hawaii. In 1989, she was selected by the Air Force Institute of Technology to attend the University of Arizona under the Airman Education and Commissioning Program where she earned the degree of Bachelor of Science in Mechanical Engineering in May 1992. Karla received her commission on 23 September 1992 upon graduation from Officer Training School. After two years as an aeronautical/mechanical systems engineer at San Antonio Air Logistics Center, Kelly AFB, Texas, she entered the School of Engineering, Air Force Institute of Technology in May 1995.

Karla is married to Daniel J. Mika and together they have been blessed with the responsibility of raising two joyful children: Jason Nathaniel [REDACTED] and Kathryn Anne [REDACTED]

[REDACTED] St
[REDACTED] IA

REPORT DOCUMENTATION PAGE

Form Approved
OMB No. 0704-0188

Public reporting burden for this collection of information is estimated to average 1 hour per response, including the time for reviewing instructions, searching existing data sources, gathering and maintaining the data needed, and completing and reviewing the collection of information. Send comments regarding this burden estimate or any other aspect of this collection of information, including suggestions for reducing this burden, to Washington Headquarters Services, Directorate for Information Operations and Reports, 1215 Jefferson Davis Highway, Suite 1204, Arlington, VA 22202-4302, and to the Office of Management and Budget, Paperwork Reduction Project (0704-0188), Washington, DC 20503.

1. AGENCY USE ONLY (Leave blank)	2. REPORT DATE December 1996	3. REPORT TYPE AND DATES COVERED Master's Thesis
----------------------------------	---------------------------------	---

4. TITLE AND SUBTITLE Investigation of Sorption Mass Transfer Models using Synthetic Soils	5. FUNDING NUMBERS
---	--------------------

6. AUTHOR(S) KARLA K. MIKA, Capt, USAF	
---	--

7. PERFORMING ORGANIZATION NAME(S) AND ADDRESS(ES) Air Force Institute of Technology (AFIT) Wright Patterson AFB, OH 45433-6583	8. PERFORMING ORGANIZATION REPORT NUMBER AFIT/GEE/ENV/96D-13
---	---

9. SPONSORING / MONITORING AGENCY NAME(S) AND ADDRESS(ES) Air Force Office of Scientific Research (AFOSR)/NA ATTN: Capt Mike Chipley Bolling AFB, Washington D.C.	10. SPONSORING / MONITORING AGENCY REPORT NUMBER
--	--

11. SUPPLEMENTARY NOTES

12a. DISTRIBUTION / AVAILABILITY STATEMENT Approved for public release; distribution unlimited	12b. DISTRIBUTION CODE
---	------------------------

13. ABSTRACT (Maximum 200 words)

Grain-scale sorption mass transfer is an important process that must be considered when predicting clean-up time and choosing remediation techniques for subsurface hazardous waste contamination. Rate-limited sorption is responsible for the rebound effect, where remediated groundwater is recontaminated by desorption. Sorbed contaminants are not available for microbial degradation, and the desorption rate may govern the effectiveness of natural attenuation by biodegradation. Grain-scale sorption nonequilibrium is generally attributed to diffusive transport, either in SOM or in mineral micropores. Typically used sorption mass transfer models either fail to reproduce long-term slow desorption (first-order models), or are based on diffusion in assumed (often spherical) grain geometries. New multisite models have been proposed that incorporate more realistic grain geometries. To validate these models, we have conducted sorption rate experiments with paraffin, nylon, and porous ceramic spheres. These synthetic surrogate soils were chosen for their differing, but known, sorption coefficients, diffusion coefficients, and geometries. Experiments were conducted in batch systems containing only a single material and size, as well as distributions of two or more materials and sizes. We tested the ability of the model to simulate the behavior of these systems and to fit system parameters from rate data.

14. SUBJECT TERMS sorption, nonequilibrium sorption, diffusion model, mass transfer, partitioning, hydrophobic organic compound, synthetic soil, batch experiment, groundwater contamination	15. NUMBER OF PAGES 120
	16. PRICE CODE

17. SECURITY CLASSIFICATION OF REPORT Unclassified	18. SECURITY CLASSIFICATION OF THIS PAGE Unclassified	19. SECURITY CLASSIFICATION OF ABSTRACT Unclassified	20. LIMITATION OF ABSTRACT UL
---	--	---	----------------------------------